Article

Targeting *Pf*Prohibitin 2-Hu-Hsp70A1A complex as a unique approach towards malaria vaccine development

Essentiality of *Pf*PHB2-Hsp70A1A in parasite invasion

siRNA — Down-regulation of Hsp70A1A

HA-*glm*S — Down-regulation of *Pf*PHB2

Reduced interaction leads to reduced invasion

Translational role

Interacting merozoites and RBC's

Anti-Hsp70A1A mAb

Novel complex of PfPHB2-Hsp70A1A

Presence of α-*Pf*PHB2 antibody in malaria infected patient

Malaria infected patient's

Anti-*Pf*PHB2 antibody detected

Translational role

Interacting merozoites and RBC's

Anti-P*f*PHB2 Ab

Reduced interaction leads to reduced invasion

Manisha Marothia,
Ankita Behl, Preeti
Maurya, ...,
Sivaprakash
Ramalingam,
Anand
Ranganathan,
Shailja Singh

anand.icgeb@gmail.com (A.R.)
shailja.jnu@gmail.com (S.S.)

Highlights

Hsp70A1A and *Pf*PHB2 were identified as novel host-parasite interacting partners

*Pf*PHB2-Hsp70A1A interaction facilitates merozoite binding and invasion

Anti-*Pf*PHB2 and Hsp70A1A antibodies inhibit Hsp70A1A-*Pf*PHB2 binding

*Pf*PHB2 antibodies in patient sera mark *Pf*PHB2 as potent vaccine candidate

Article

Targeting *Pf*Prohibitin 2-Hu-Hsp70A1A complex as a unique approach towards malaria vaccine development

Manisha Marothia,[1,10] Ankita Behl,[1,10] Preeti Maurya,[1,10] Monika Saini,[1,10] Rumaisha Shoaib,[2,10] Swati Garg,[1] Geeta Kumari,[1] Shreeja Biswas,[1] Akshay Munjal,[1] Sakshi Anand,[1] Amandeep Kaur Kahlon,[1] Pragya Gupta,[3] Saurav Biswas,[4] Bidhan Goswami,[5] Haider Thaer Abdulhameed Almuqdadi,[2,6] Ipsita Pal Bhowmick,[4] Maxim Shevtsov,[7,8,9] Sivaprakash Ramalingam,[3] Anand Ranganathan,[1,*] and Shailja Singh[1,11,*]

SUMMARY

Malaria parasite invasion to host erythrocytes is mediated by multiple interactions between merozoite ligands and erythrocyte receptors that contribute toward the development of disease pathology. Here, we report a novel antigen *Plasmodium* prohibitin "*Pf*PHB2" and identify its cognate partner "Hsp70A1A" in host erythrocyte that plays a crucial role in mediating host-parasite interaction during merozoite invasion. Using small interfering RNA (siRNA)- and glucosamine-6-phosphate riboswitch (glmS) ribozyme-mediated approach, we show that loss of Hsp70A1A in red blood cells (RBCs) or *Pf*PHB2 in infected red blood cells (iRBCs), respectively, inhibit *Pf*PHB2-Hsp70A1A interaction leading to invasion inhibition. Antibodies targeting *Pf*PHB2 and monoclonal antibody therapeutics against Hsp70A1A efficiently block parasite invasion. Recombinant *Pf*PHB2 binds to RBCs which is inhibited by anti-*Pf*PHB2 antibody and monoclonal antibody against Hsp70A1A. The validation of *Pf*PHB2 to serve as antigen is further supported by detection of anti-*Pf*PHB2 antibody in patient sera. Overall, this study proposes *Pf*PHB2 as vaccine candidate and highlights the use of monoclonal antibody therapeutics for future malaria treatment.

INTRODUCTION

The rapid development of drug resistance is culpable for perpetual threat of malaria on mankind and is indicated by numerous cases and deaths in the year 2022.[1] The insensitivity of the malaria parasite toward the current therapies and lack of equipotent drugs for malaria treatment call for an urgent need for discovering parasite-specific drugs and vaccine candidates.[2]

Prohibitins (PHBs) are a highly conserved class of proteins that are ubiquitously expressed and have been reported to be present in the mitochondria, nucleus, and cytosol.[3] The evolutionary conserved PHBs belong to a stomatin-PHB flotillin-HflC/K (SPFH) superfamily, bearing the common PHB domain.[3,4] The members of this superfamily are found in all eukaryotic cells, bacteria, and archaea, and they are usually anchored to cell membranes in eukaryotic cells, including mitochondrial membranes.[3,5] The multi-meric complex of PHB1 and PHB2 located in the inner membrane of the mitochondria exerts regulatory functions by acting as chaperones for other proteins.[6] The two members of the PHB family, PHB1 and PHB2, are highly homologous to each other and share more than 50% identical amino acid residue.[7] Hydrophobic stretches at the amino terminal end anchor PHB1 and PHB2 to the membrane, while large carboxy terminal domains of ∼30 kDa are exposed to the intermembrane space. These domains consist of a so-called PHB domain, characteristic of the SPFH family of membrane proteins, and a predicted coiled-coil region at the carboxy terminal end, which is crucial for the assembly of PHB complexes.[8] The large membrane-bound complexes of PHB1 and PHB2 are composed of multiple copies of PHB1 and PHB2 subunits and possess a native molecular mass of >1 MDa[9]

PHBs have been reported to elicit multiple functions that may be defined by their cellular localization and cell type.[7,9] The multiple functions attributed to PHBs include nuclear transcription, tumorigenesis, plasma membrane lipid scaffold protein, and a regulator of

[1]Special Centre for Molecular Medicine, Jawaharlal Nehru University, New Delhi, India
[2]Department of Bioscience, Jamia Millia Islamia, New Delhi, India
[3]CSIR-Institute of Genomics and Integrative Biology, Mathura Road, Sukhdev Vihar, New Delhi 110025, India
[4]Regional Medical Research Center-Northeast Region (RMRC-NE)-ICMR, Dibrugarh 786001, India
[5]Multidisciplinary Research Unit, Agartala Government Medical College, Agartala, Tripura (West), India
[6]Department of Chemistry, College of Science, Al-Nahrain University, Baghdad, Iraq
[7]Klinikum rechts der Isar, Technical University of Munich, 81675 Munich, Germany
[8]Institute of Cytology of the Russian Academy of Sciences (RAS), 194064 St. Petersburg, Russia
[9]Personalized Medicine Centre, Almazov National Medical Research Centre, Akkuratova Str. 2, 197341 St. Petersburg, Russia
[10]These authors contributed equally
[11]Lead contact
*Correspondence: anand.icgeb@gmail.com (A.R.), shailja.jnu@gmail.com (S.S.)
https://doi.org/10.1016/j.isci.2024.109918

mitochondrial morphogenesis and apoptosis in the mitochondria.[7,9] Hence, due to their ability to perform numerous functions, PHBs have been regarded as potential targets for therapeutic interventions.[10] Despite these diverse biological roles in eukaryotes, bacteria, and archaea, the role of PHB proteins in *Plasmodium* is poorly understood.

A recent report on PHB of *Leishmania donovani* has shown its upregulated expression in infective metacyclic promastigotes and that it binds with macrophage surface Hsp70 to mediate host-parasite interaction.[11] Anti-PHB antibodies were identified in visceral leishmaniasis patients that suggest the potential of *Leishmania donovani* PHB to generate humoral response in humans.[11] Hsp70 refers to a family of heat shock proteins that play an essential role in cellular protection and stress response. Hsp70 proteins are known as molecular chaperones owing to their ability to assist in folding, assembly, and transport of proteins within cells.[12] They are involved in maintaining protein homeostasis (i.e., proteostasis), preventing protein misfolding, and aiding in the refolding of damaged proteins. Hsp70 proteins expression is induced in response to various stress conditions, including heat shock, hypoxia, glucose deprivation, low pH, etc. They help cells survive under adverse conditions by preventing the accumulation of misfolded or aggregated proteins, which can be toxic to cells.[12] Interestingly, Hsp70 family of proteins is known to play critical role in malaria parasite survival and disease pathogenicity.[13]

Our previous study demonstrated that *Pf*PHB1 (PlasmoDB Id: PF3D7_0829200) and *Pf*PHB2 (PlasmoDB Id: PF3D7_1014700) are expressed during sexual and asexual blood stages of the parasite.[14] Rocaglamide (Roc-A), a known inhibitor of PHBs and anti-cancerous agent, showed anti-malarial activity against asexual-blood-stage malaria parasite and also attenuates transmission-stage parasite (gametocytes) and oocyst growth with significant morphological aberrations.[14] Here, we have attempted to delineate the function of *Plasmodium falciparum* PHBs and identified human Hsp70A1A as one of the host proteins with which *Pf*PHB2 interacts. We show for the first time that *Pf*PHB2 is localized to parasite surface and mediates host-parasite interaction during merozoite invasion to RBCs. Small interfering RNA (siRNA)- and glmS ribozyme-mediated downregulation of Hsp70A1A and *Pf*PHB2, respectively, abrogates the capability of the parasites to bind to red blood cells (RBCs). Anti-*Pf*PHB2 antisera and anti-Hsp70A1A monoclonal antibodies inhibit *Pf*PHB2- RBC binding and attenuate merozoite invasion, further suggesting *Pf*PHB2-Hsp70A1A pair as an important entity in host-parasite interactions. Interestingly, we observed the presence of anti-*Pf*PHB2 antibodies in malaria patients which depict that *Plasmodium falciparum* PHB 2 is able to generate a strong humoral response in humans. Overall, our data highlight *Pf* PHB as a potentially important candidate involved in host-parasite interactions and provide a platform to target *Pf*PHB2-Hsp70A1A complex for the development of highly effective and durable vaccines against the human malaria parasites.

RESULTS

Bacterial two-hybrid approach depicts host Hsp70A1A as a cognate partner of *Pf*PHB2

Sequence analysis and domain organization using Blastp[15] depicted that *Pf*PHB1 and *Pf*PHB2 harbors a PHB domain that forms the hallmark of SPFH superfamily (Figure 1A). We next explored the presence of *Pf*PHB1 and *Pf*PHB2 homologs in other species using organism-specific Blastp search in *Leishmania major*, *Saccharomyces cerevisiae*, *Arabidopsis thaliana*, *Drosophila melanogaster*, *Mus musculus*, and *Homo sapiens*. Multiple sequence alignment using Clustal Omega[16] revealed highly conserved nature of *Pf*PHB1 and *Pf*PHB2 with their homologs in other species (Figures S1 and S2).

Since PHBs are supposed to perform moonlighting functions, we first attempted to look for new host RBC and *Plasmodium* interactions by using a bacterial two-hybrid approach and screened a human cDNA library against *Pf*PHB1 and *Pf*PHB2. On the basis of blue-white selection, a putative colony positive for interaction was selected for *Pf*PHB2 and the isolated DNA sequenced (Figure 1B i). Sequence analysis showed substrate-binding domain (SBD; 383–508 aa) of Hsp70A1A as a possible host-interacting partner for *Pf*PHB2. The plasmids harbored in the selected colony were segregated, confirmed by PCR, and used to co-transform competent R1 *Escherichia coli* cells to verify the interaction. Two-hybrid plasmids expressing the *Mycobacterium tuberculosis* proteins ESAT6 and CFP10, and whose interaction has been well documented previously,[17] acted as the positive control for the assay (Figure 1B i). The physical parameters of Hsp70A1A and *Pf*PHB2 further comply with their structural interactive compatibility. The acidic isoelectric point (pI) of Hsp70A1A ∼5.5 and the basicity of *Pf*PHB2 ∼ 9.72 pI further mark them as possible interacting partners (Figure 1B ii). *Pf*PHB1 did not showed interaction with Hsp70A1A which depicts the specificity of the assay.

For a quantitative estimation of the strength of interaction between *Pf*PHB2 and Hsp70A1A, liquid β-galactosidase assay was performed (Figure 1B iii). The enzyme activity in case of *Pf*PHB2 and Hsp70A1A interaction was found to be comparable to that of CFP10 and ESAT6 interaction pair which are well documented to form a tight heterodimer.[17] pBTnn/pTRG-ESAT6, and *Pf*PHB1/Hsp70A1A marked as negative controls by showing negligible enzymatic activity (Figure 1B iii). Overall, the data suggest potential functional interaction of *Pf*PHB2 with human Hsp70A1A.

Recombinant *Pf*PHB2 interacts with Hsp70A1A with a K_d of 1.16 µM

On the basis of our bacterial two-hybrid results, we attempted to further explore the possibility of *Pf*PHB2 and Hsp70A1A interaction, by using *in silico* docking studies of *Pf*PHB2-Hsp70A1A pair followed by *in vitro* binding studies. Sequence analysis and domain organization using Blastp depicted that human Hsp70A1A possesses two domains viz. an N-terminal nucleotide-binding domain (NBD) with ATPase activity, which is connected by a linker region to a C-terminally located SBD (Figure 2A i). Alpha fold models of *Pf*PHB1 and *Pf*PHB2 were retrieved from AlphaFold Protein structure database[18] and were used to dock with crystal structure of SBD of Hsp70A1A (PDB ID: 4WV5) using PIPER module of Schrodinger Maestro (Schrodinger, LLC, NY, USA, 2009) to investigate their interaction at structural level. We observed that *Pf*PHB2 binds well into the cavity of SBD of Hsp70A1A with a binding energy of −1241.236 kcal/mol (Figure 2A ii). Detailed residue analysis reveals that Ser 60 and Arg 75 constituting PHB domain of *Pf*PHB2 form hydrogen bonds with Arg 535 and Asp 433 of Hsp70A1A, respectively
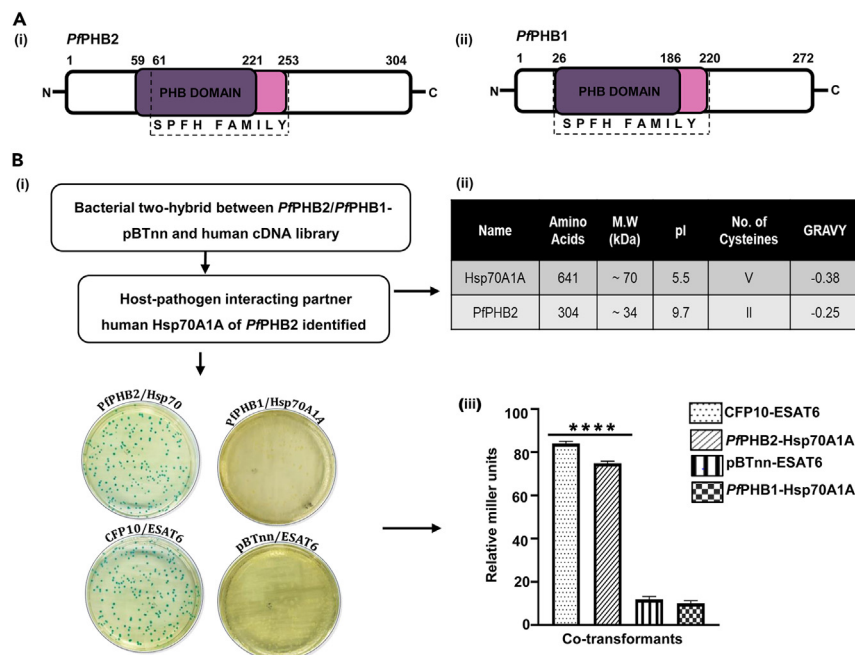
Figure 1. Domain organization and bait two-hybrid analysis between human cDNA library and *Pf*PHB1/PfPHB2

(A) Schematic representation of predicted domains of *Pf*PHB (i) and *Pf*PHB (ii). Stomatin-prohibitin flotillin-HflC/K (SPFH) superfamily bearing the common PHB domain is depicted.

(B) (i) X-gal indicator plate of bacterial two-hybrid experiment between human cDNA library and *Pf*PHB1 and *Pf*PHB2. Plates are labeled to represent genes cloned in pTRG/pBTnn. ESAT6pTRGnn/CFP10pBTnn is the positive control while ESAT6/empty pBTnn is the negative control. (ii) Protein parameters highlighting length, molecular weight (MW), isoelectric point (pI), number of cysteines, and grand average of hydropathicity (GRAVY) of the identified host-pathogen protein interactors. (iii) Liquid β-galactosidase assay for quantitative estimation of interaction strength between *Pf*PHB2 and Hsp70A1A compared to that with positive and negative controls. Co-transformants ESAT6pTRGnn/CFP10pBTnn and ESAT6/empty pBTnn were taken as positive and negative control, respectively. Enzyme activity is expressed in terms of Miller units. The graph is the average of three independent assays, and standard deviation is represented by error bars. Statistical analysis was performed using unpaired t test and is shown with p values ≤ 0.0001****.

(Figure 2A iii). Also Arg 458 of Hsp70A1A was found to form two hydrogen bonds with Ala 41 and Thr 42 of *Pf*PHB2 (Figure 2A iii). On the contrary, *Pf*PHB1 dock poorly to SBD of Hsp70A1A by forming only a single hydrogen bond between GLN 426 of Hsp70A1A and ARG 40 of *Pf*PHB1 (Figure S3). To further validate this interaction, we expressed and purified full-length construct of human Hsp70A1A in bacterial expression system. Codon-optimized gene of Hsp70A1A was synthesized commercially from GenScript USA and subcloned in pMTSAra vector. The recombinant protein (~70 kDa) was purified using Ni-NTA affinity chromatography (Figure 2B i). Identity of recombinant Hsp70A1A was checked by western blotting using anti-histidine antibodies (Figure 2B ii). Recombinant *Pf*PHB1 and *Pf*PHB2 were purified for experiments as previously described.[14] Purified *Pf*PHB1 and *Pf*PHB2 run as species of approximately 30.6 and 34.5 kDa, respectively on SDS-PAGE (Figure 2B iii, iv). A far-UV circular dichroism (CD) spectrum on Hsp70A1A, *Pf*PHB1, and *Pf*PHB2 was collected that depicts the correctly folded state of recombinant proteins (Figure S4).

Binding studies were performed using dot blot assays where *Pf*PHB1 and *Pf*PHB2 were immobilized on nitrocellulose (NC) membrane and incubated with recombinant Hsp70A1A before probing with anti-Hsp70A1A monoclonal antibody. Our data showed that *Pf*PHB2 binds with Hsp70A1A, whereas no interaction was observed for *Pf*PHB1 with Hsp70A1A (Figure 2C). Hsp70A1A did not bind BSA (negative control), which depicts the specificity of the assay. Integrated density analysis of each dot further demonstrated significant binding of *Pf*PHB2 with Hsp70A1A (Figure 2C). *Pf*PHB2-Hsp70A1A binding was also investigated using indirect ELISA assays which reveal significant and specific interaction of *Pf*PHB2 with host Hsp70A1A in a concentration-dependent manner that saturated at higher concentrations (Figure 2D). We next employed microscale thermophoresis (MST) to study the kinetic analysis of one-to-one interaction of purified recombinant *Pf*PHB2 with Hsp70A1A using NanoTemper Monolith NT.115 instrument. Here, Hsp70A1A was labeled and *Pf*PHB2 was serially diluted with maximum concentration at 25 μM. Figure 2E i shows dose-response curve for *Pf*PHB2-Hsp70A1A binding. K_d for *Pf*PHB2-Hsp70A1A binding was observed to be 1.16 ± 0.5 μM. Since our *in silico* docking studies showed interaction interface to lie at SBD of Hsp70A1A, we cloned this region in pMTSAra vector and purified recombinant protein using nickel-nitriloacetic acid (Ni-NTA) chromatography (Figure S5 i) to test its binding with *Pf*PHB2. Identity of recombinant Hsp70A1A-SBD construct was analyzed by immunoblotting using anti-histidine antibodies (Figure S5ii). CD data of Hsp70A1A-SBD depicted correctly folded state of protein construct (Figure S5iii). Our MST data showed that *Pf*PHB2 interacts with Hsp70A1A-SBD construct with a K_d value of 2.38 ± 0.8 μM (Figure 2E ii). These results suggest that *Pf*PHB2-Hsp70A1A interaction is primarily mediated by SBD of Hsp70A1A. Plots representing MST data of *Pf*PHB1 with Hsp70A1A as a negative control are shown in Figure 2E ii.
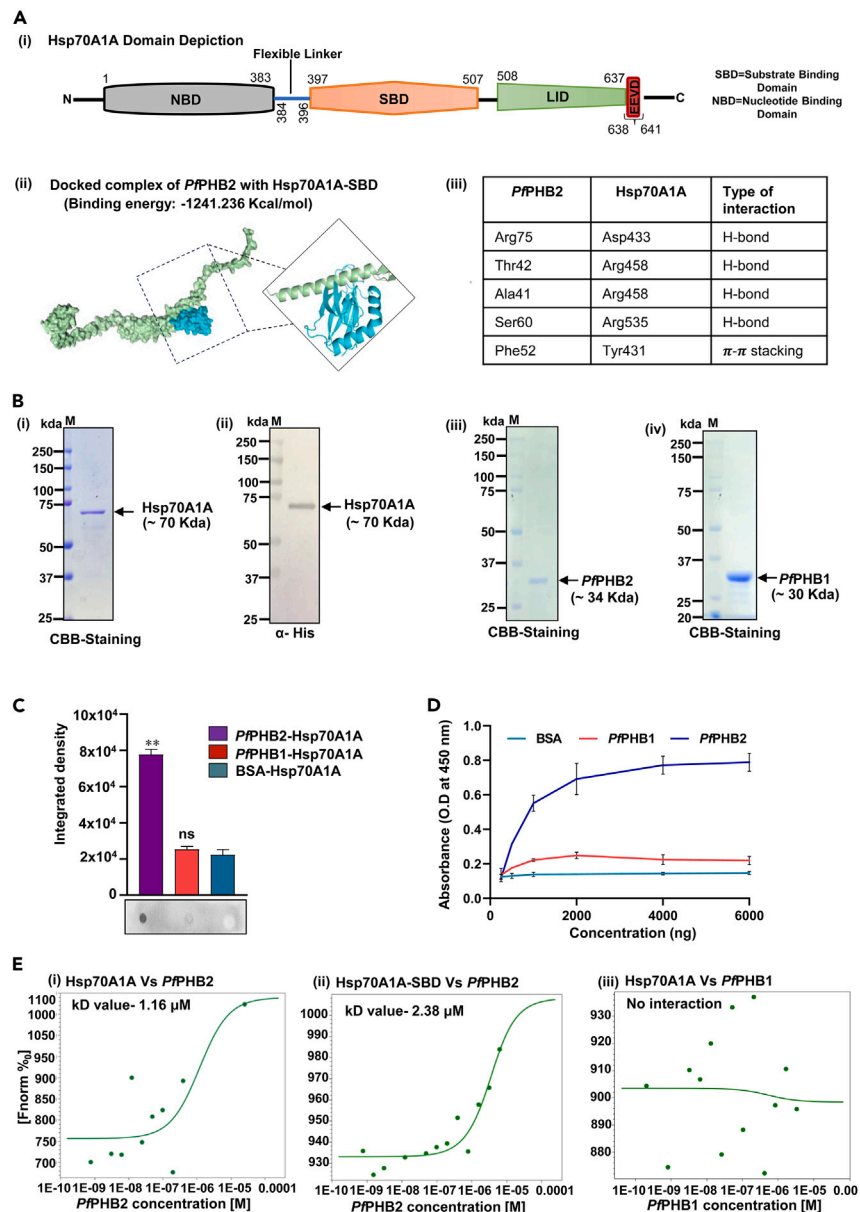
Figure 2. *In silico* docking of *Pf*PHB2 with Hsp70A1A and their interaction analysis using dot blot, indirect ELISA, and MST

(A i) Schematic representation of predicted domains and motifs of Hsp70A1A. Domains/motifs are labeled on the scheme. (A ii) Surface representation of *Pf*PHB2-Hsp70A1A docked complex representing interacting interface of both proteins. *Pf*PHB2 is represented in green color and SBD of human Hsp70A1A is represented in cyan color. (A iii) Table representing the interaction interface residues of *Pf*PHB2-Hsp70A1A docked complex.

(B i) SDS-PAGE showing recombinant purified Hsp70A1A tagged with 6x-Histidine and stained with Coomassie brilliant blue (CBB). (B ii) Western blot analysis of recombinant purified Hsp70A1A probed with anti-histidine antibodies. (B iii, iv) SDS-PAGE showing recombinant purified *Pf*PHB2 (iii) and *Pf*PHB1 (iv) tagged with 6x-Histidine and stained with Coomassie brilliant blue (CBB).

(C) Dot blot assays showing the interaction of *Pf*PHB2 with Hsp70A1A. 5 μg each of *Pf*PHB1, *Pf*PHB2 and BSA were spotted, hybridized with Hsp70A1A, and probed using anti-Hsp70A1A monoclonal antibodies (1:5,000). Bar diagram shows plots of intensity measurements from three replicates in an experiment using ImageJ software. "*" represents statistical significance at $p < 0.05$ relative to BSA. A representative blot from each set is shown.

(D) Semi-quantitative ELISA depicting concentration-dependent binding curves of Hsp70A1A with *Pf*PHB2 where y axis represents absorbance at 450 nm and x axis denotes amount of Hsp70A1A. Error bars represent standard deviation among three replicates.

(E) Interaction studies of *Pf*PHB2 with Hsp70A1A (i) and Hsp70A1A-SBD (ii) using MST. Labeled Hsp70A1A and Hsp70A1A-SBD was titrated against varying concentrations of *Pf*PHB2 Dose-response curve was generated that resulted in K_d value of 1.16 μM and 2.38 μM for *Pf*PHB2-Hsp70A1A interaction. (iii) Plot represents MST data of *Pf*PHB1 with Hsp70A1A as a negative control.
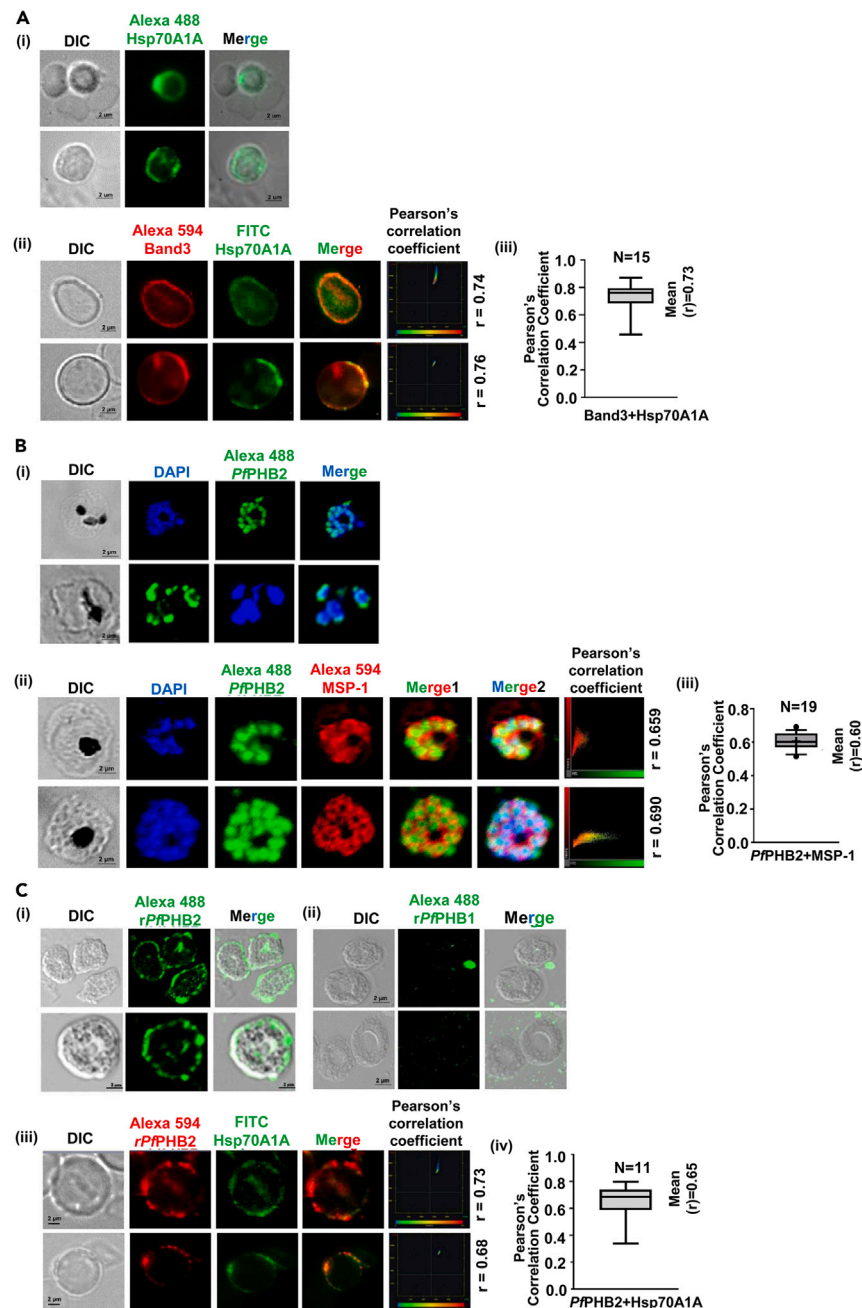
Figure 3. Localization and receptor-ligand interaction studies of *Pf*PHB2-Hsp70A1A pair

(A i) Localization of Hsp70A1A on human erythrocytes. RBCs were incubated with anti-Hsp70A1A monoclonal antibody followed by secondary Alexa Fluor 488-conjugated goat anti-mouse IgG antibody (1:500). DIC: differential interference contrast image, Hsp70A1A: mouse anti- Hsp70A1A (green); merge: overlay of Hsp70A1A with DIC (Scale bar: 2 μm). (A ii) Co-localization of Hsp70A1A with Band 3 on human erythrocytes. RBCs were incubated with anti-Hsp70A1A-fluorescein isothiocyanate (FITC)-labeled monoclonal antibody and mice anti-Band 3 primary antibodies (1:200) followed by Alexa Fluor 594-conjugated anti-mice (1:500, red color) as secondary antibodies. DIC: differential interference contrast image, Hsp70A1A: anti- Hsp70A1A (green); Band 3: mouse anti-Band 3 (red), merge: overlay of Hsp70A1A with Band 3 (Scale bar: 2 μm). Plots representing Pearson's correlation coefficient (r) of represented images are shown. (A iii) Plot represents mean Pearson's correlation coefficient (r) of *n* = 15 for Hsp70A1A co-localization with Band 3.

(B i) Localization analysis of *Pf*PHB2 in infected erythrocytes. Smears of methanol-fixed *Pf*3D7-infected erythrocytes were stained with *Pf*PHB2 antibodies (1:250) followed by incubation with Alexa Fluor-conjugated secondary antibodies (Alexa Fluor 488, green). DIC: differential interference contrast image, DAPI: nuclear staining 40, 6-diamidino-2-phenylindole (blue); *Pf*PHB2: mouse anti-*Pf*PHB2 (green); merge: overlay of *Pf*PHB2 with DAPI (Scale bar: 2 μm). (B ii) Co-localization of *Pf*PHB2 in merozoite stage with *Pf* merozoite surface protein 1 (MSP-1). DIC: differential interference contrast image, DAPI: nuclear staining 40, 6-diamidino-2-phenylindole (blue); *Pf*PHB2: mouse anti-*Pf*PHB2 (green); *Pf*MSP1: rabbit anti-MSP1 (red), merge 1: overlay of *Pf*PHB2 with *Pf*MSP1, merge 2: overlay of *Pf*PHB2

Figure 3. *Continued*

with *Pf*MSP1 and DAPI (Scale bar: 2 μm). Plots representing Pearson's correlation coefficient (r) of represented images are shown. (B iii) Plot represents mean Pearson's correlation coefficient (r) of *n* = 19 for *Pf*PHB2 co-localization with *Pf*MSP1.

(C i, ii) Binding of recombinant *Pf*PHB2 (i) and *Pf*PHB1 (ii) to human erythrocytes. RBCs were incubated with 10 μM recombinant *Pf*PHB2 and *Pf*PHB1 separately for 2 h followed by incubation with anti-*Pf*PHB2 and anti-*Pf*PHB1 antibody, respectively. RBCs were stained with Alexa Fluor 488-conjugated goat anti-mouse IgG antibody (1:200; green) against primary antibody followed by confocal microscopy. DIC: differential interference contrast image, recombinant *Pf*PHB2: mouse anti-*Pf*PHB2 (green); merge: overlay of recombinant *Pf*PHB2 with DIC Scale bar = 2 μm. (C iii) Co-localization of recombinant *Pf*PHB2 with native Hsp70A1A. Here anti-Hsp70A1A-FITC-conjugated monoclonal antibody (1:300) were used. DIC: differential interference contrast image, recombinant *Pf*PHB2: mouse anti-*Pf*PHB2 (green); Native Hsp70A1A: anti-Hsp70A1A-FITC conjugated, merge: overlay of recombinant *Pf*PHB2 with native Hsp70A1A. (Scale bar = 2 μm). Plots representing Pearson's correlation coefficient (r) of represented images are shown. (C iv) Plot represents mean Pearson's correlation coefficient (r) of *n* = 11 for recombinant *Pf*PHB2 co-localization with Hsp70A1A.

*Pf*PHB2 acts as a ligand for host Hsp70A1A for merozoite binding and invasion

To get insights into the functional aspect of *Pf*PHB2-Hsp70A1A binding, we first investigated the localization of host Hsp70A1A on RBCs. Our immunolocalization analysis using anti-Hsp70A1A monoclonal antibody demonstrated the expression of Hsp70A1A on the RBC surface (Figure 3A i). Surface localization of Hsp70A1A was further confirmed by using Band 3 as marker protein for RBC surface. Hsp70A1A showed co-localization with Band 3, suggestive of its surface localization (Figure 3A ii, iii). Next the expression of *Pf*PHB2 during the asexual blood stages of *Pf*3D7 was investigated by indirect immunofluorescence assays (IFA) using anti-*Pf*PHB2 antibodies. Thin blood smears of mixed-stage *Pf*3D7 cultures were fixed with methanol and blocked with 5% BSA in PBS. The slides were probed with anti- *Pf*PHB2 antibodies (1:300) followed by Alexa Fluor 488-conjugated anti-mice secondary antibodies (1:500). The parasite nuclei were counterstained with DAPI (4′,6′-diamidino-2-phenylindole). Fluorescence pattern observed for *Pf*PHB2 at asexual blood stages was suggestive of its localization to parasite surface (Figure 3B i). To ascertain the localization of *Pf*PHB2, we performed co-staining with *Pf*MSP1 as parasite surface marker protein. Our data demonstrate that *Pf*PHB2 significantly co-localizes with *Pf*MSP1, further suggesting its surface localization (Figure 3B ii, iii).

Next we performed RBC binding assay with recombinant *Pf*PHB2 to evaluate the possibility of receptor-ligand interaction of *Pf*PHB2-Hsp70A1A pair. Uninfected human erythrocytes were incubated with recombinant *Pf*PHB2 (10 μg) followed by fixation with PFG (4% paraformaldehyde +0.0075% glutaraldehyde) and subsequent blocking with 5% BSA. Cells were incubated with anti-*Pf*PHB2 mice sera (1:300) followed by anti-mice Alexa Fluor 488 secondary antibody (1:500). Our results suggested significant localization of bound *Pf*PHB2 around the RBC membrane (Figure 3C i). No fluorescence signal around the RBCs was observed when *Pf*PHB1 was incubated with RBCs (negative control; Figure 3Cii). Bound *Pf*PHB2 also co-localized with native Hsp70A1A (Figure 3Ciii, iv), further indicating that *Pf*PHB2 can act as a ligand for host receptor protein Hsp70A1A during the process of merozoite binding and invasion.

siRNA-mediated knockdown of host Hsp70A1A in erythroid progenitor cells blocks merozoite invasion

To study the functional essentiality of host Hsp70A1A during the life cycle of malaria parasite, we inhibited host Hsp70A1A expression in erythroid progenitor cells (EPCs). EPCs are erythroid progenitor cells that are known to support merozoite invasion.[19] Downregulation of Hsp70A1A expression in EPCs was performed using siRNA at different concentrations (100 nM and 250 nM), and Hsp70 expression in these transfected cells was detected by immunofluorescence assay at 72 h post-transfection. Our results indicated a significant reduction in Hsp70A1A protein expression in Hsp70A1A-specific siRNA-transfected cells as compared to untransfected cells (control) (Figure 4Ai, ii, iii). Figure 4A iv represents mean fluorescence intensity in untransfected and Hsp70A1A-specific siRNA-transfected cells. We then performed invasion inhibition assay by incubating siRNA-transfected cells with mature schizonts for 24 h. Formation of rings in these cells was evaluated. The data suggest significantly reduced number of new rings in transfected cells (Figure 4B I). Giemsa-stained images in siRNA-transfected and untransfected cells are shown in Figure 4B ii. These findings clearly demonstrate the role of host Hsp70 as a receptor involved in parasite invasion.

Inducible knockdown of *Pf*PHB2 using glmS ribozyme in *Plasmodium falciparum* impairs parasite growth

We next attempted to precisely investigate the role of *Pf*PHB2 protein in parasite growth by generating knockdown mutants of this protein using the glmS system. Here, downregulation at the mRNA level is achieved, resulting in a reduced protein synthesis of the target protein. The line was generated through integration of the glmS ribozyme into the 3′ UTR of the *Pf*PHB2 locus, allowing for post-transcriptional regulation of gene expression as previously described by Prommana et al.[20] (Figure 5A). When glucosamine (GlcN) is added, the ribozyme is cleaved leading to degradation of the mRNA and a corresponding reduction in protein expression. Selected regions of *Pf*PHB2 (38–912) were successfully cloned in hemagglutinin (HA)-glmS vector using specific primers (Figure S6A) and transfected in *P. falciparum* cultures. The positive clones were confirmed by plasmid restriction digestion (Figure S6B) and nucleotide sequencing (Figure S7 i). After a few weeks, Giemsa-stained smears showed growth of *Pf*PHB2-HA-glmS. Genomic DNA was isolated from these cultures, and PCR was used to demonstrate plasmid uptake and check for integration with combination of specific primer pairs (Figure S7ii). Reduced *Pf*PHB2 levels in knockdown line were confirmed by western blotting using anti-*Pf*PHB2 antibodies (Figure 5 Bi, ii). We then performed growth inhibition assay in *Pf*PHB2-HA-glmS line to assess the effect of *Pf*PHB2 knockdown on parasite growth. Parasite cultures were grown in the presence or absence of GlcN for 96 h, and parasitemia was counted using Giemsa-stained smears of parasite cultures. Parasite growth was found to be significantly reduced after application of GlcN (2.5 mM) relative to that in the absence of GlcN (0 mM) (Figure 5C). These data indicate that *Pf*PHB2 plays a critical role in parasite growth and survival during its life cycle in human host.
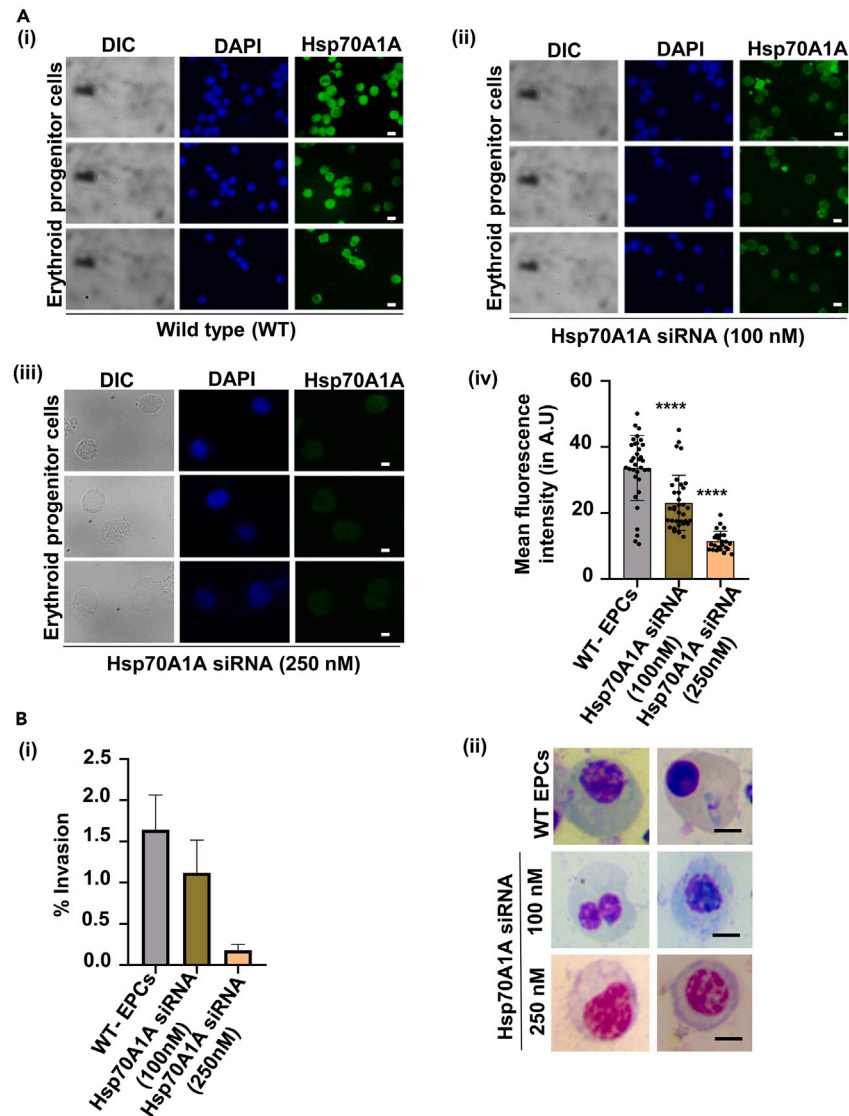
Figure 4. Downregulation of human Hsp70A1A by siRNA in erythroid progenitor cells (EPCs)

(A i, ii, iii) Expression of human Hsp70A1A was detected by IFA in wild-type (WT) EPCs (i) and those transfected with siRNA targeting Hsp70A1A mRNA at 100 nM (ii) and 250 nM concentration (iii). DIC: differential interference contrast image, DAPI: nuclear staining 40, 6-diamidino-2-phenylindole (blue); Hsp70A1A: mouse anti-Hsp70A1A (green); Scale bar: 2 μm (A iv) Intensity of Hsp70A1A staining in EPCs under each condition is shown as an intensity graph ($p < 0.0001$****).

(B i) Graph representing percentage invasion of malaria parasite in EPCs and those transfected with siRNA targeting Hsp70A1A mRNA at 100 nM and 250 nM concentration. The graph is the average of triplicate values and standard deviation is represented by error bars. (B ii) Giemsa-stained images of *Pf*3D7 in wild-type (WT) EPCs and those transfected with siRNA targeting Hsp70A1A mRNA at 100 nM and 250 nM concentration. Scale Bar represents 5 μm.

Antibodies targeting Hsp70A1A and *Pf*PHB2 inhibit parasite-RBC binding and block merozoite invasion

We next performed antibody neutralization assays to examine the effect of anti-Hsp70A1A monoclonal antibody and anti-*Pf*PHB2 antibodies on recombinant *Pf*PHB2 binding to RBCs. In the first set of experiments, anti-*Pf*PHB2 (1:50) mice sera was incubated with 10 μg of recombinant *Pf*PHB2 and then allowed to bind with RBCs. In the other set of experiments, anti-Hsp70A1A monoclonal antibodies were incubated with RBCs followed by incubation with recombinant *Pf*PHB2. Immunolocalization analysis in both sets of experiments using anti-*Pf*PHB2 antibody depicted no binding of recombinant *Pf*PHB2 to RBC surface (Figure 6Ai, ii). Direct binding of recombinant *Pf*PHB2 to RBCs was taken as positive control in the assay (Figure 6A iii). These data suggest that anti-Hsp70A1A and anti-*Pf*PHB2 antibodies can inhibit parasite binding to RBCs that is mediated by *Pf*PHB2-Hsp70A1A interaction pair. Figure 6A iv represents mean fluorescence intensity in anti-Hsp70A1A monoclonal antibody- and anti-*Pf*PHB2 antibodies-treated samples along with the positive control.

Further, anti-Hsp70A1A and anti-*Pf*PHB2 antibodies were tested for inhibition of parasite invasion into normal erythrocytes by *P. falciparum*. The invasion assays were carried out in erythrocytes in the presence of heat-inactivated *Pf*PHB1/*Pf*PHB2 antisera at a dilution
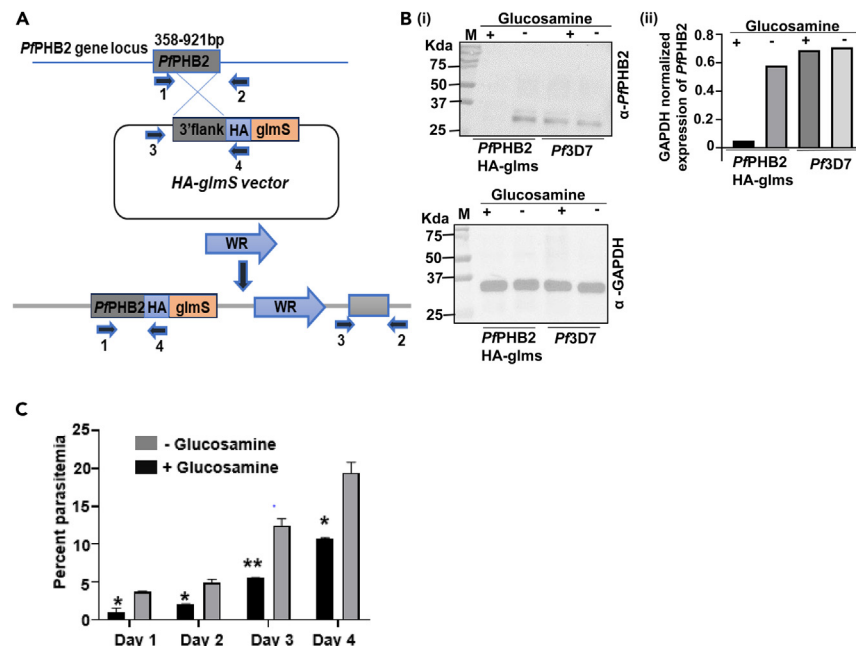
Figure 5. glmS ribozyme mediated knockdown of *Pf*PHB2 in malaria parasite

(A) Schematic representation of HA-glmS reverse genetic approach showing the integration of *Pf*PHB2-HA -glmS plasmid at the C terminus of the endogenous *Pf*PHB2 gene locus. The numbered arrows represent the primers used for plasmid uptake and integration check.

(B i) Upper panel: western blot showing the reduced *Pf*PHB2 levels in *Pf*PHB2-HA-glmS knockdown line in presence of 2.5 mM glucosamine (+GlcN) as compared to control (-GlcN). *Pf*PHB2 levels in *Pf*3D7 treated with and without GlcN are also depicted. Lower panel: western blot representing GAPDH as loading control. (B ii) Bar diagram showing plots of intensity measurements of *Pf*PHB2 in HA-glmS knockdown line in presence of 2.5 mM glucosamine (+GlcN) as compared to control (-GlcN). *Pf*PHB2 levels in *Pf*3D7 treated with and without GlcN are also quantified and depicted. Quantified *Pf*PHB2 protein levels were normalized against GAPDH protein levels.

(C) Graph showing *Pf*PHB2-HA-glmS parasite growth in presence of 2.5 mM glucosamine (+GlcN) as compared to control (-GlcN). Tightly synchronized ring-stage parasite culture of transgenic parasites grown with or without glucosamine, and their growth was monitored for 96 h. The p values were calculated by Student's t test (p values $\leq$0.05 *, p value $\leq$0.01**).

of 1:5 and 1:10. Similarly anti-Hsp70A1A monoclonal antibodies were tested for invasion inhibition at different concentrations (0.25, 0.5, 0.75, and 1 mg/mL). Our results revealed that antisera against *Pf*PHB2 and anti-Hsp70A1A monoclonal antibodies significantly reduced the invasion (Figure 6 Bi, Ci) while *Pf*PHB1 antisera has no significant effect upon the invasion process (Figure 6B i). An invasion inhibition of 78% and 60% was observed in the presence of *Pf*PHB2 antisera at a dilution of 1:5 and 1: 10 (Figure 6B i). Giemsa-stained images showing reduced invasion in treated and control samples are shown in figure 6Bii, C ii. These data clearly depict the role of host Hsp70-*Pf*PHB2 pair during merozoite invasion and that their antibodies can inhibit this critical event that occurs during the life cycle of malaria parasite.

Sera from malaria-infected patients show the presence of anti-*Pf*PHB2 antibodies that can block *Pf*PHB2-Hsp70A1A interaction and attenuate parasite growth

Several *Pf* proteins have been identified as antigens generating antibodies in malaria patients,[21] which makes them important for diagnostic markers as well as possible vaccine candidates. Our results indicate that *Pf*PHB2 binds to Hsp70A1A on the RBC membrane and participates in merozoite invasion. In line with the aforementioned facts, we looked at clinical and therapeutic importance of this protein and investigated the presence of *Pf*PHB2 antibodies in patient sera using ELISA-based assay. 1,000 ng of recombinant *Pf*PHB2 along with *Pf*PHB1 and BSA were coated on ELISA plates and blocked with 5% BSA in PBS. Coated wells were treated with three different patient sera (1:1,000; P1, P2, P3) followed by secondary human horseradish peroxidase (HRP)-conjugated antibody (1:10,000). The antisera used were from patients whose disease profile was characterized by standardized assays for malaria. Details of patients whose sera were used for the experiment are given in Table S1. We found that reactivity of recombinant *Pf*PHB2 to the patient sera was significant in all three samples tested (Figure 7A i) while negligible reactivity of recombinant *Pf*PHB1 and BSA was observed. This part of the data therefore showed that *Pf*PHB2 is able to elicit antibodies in malaria patients.

Based on these findings, we investigated the presence of *Pf*PHB2 antibody in all available patient samples (P1-P10) along with three naive uninfected samples. Interestingly, reactivity of recombinant *Pf*PHB2 to the sera was significant in all samples tested (Figure 7A ii). However, varied levels of sera reactivity were observed as the level of infectivity can differ in patients. No significant reactivity of recombinant *Pf*PHB2 to
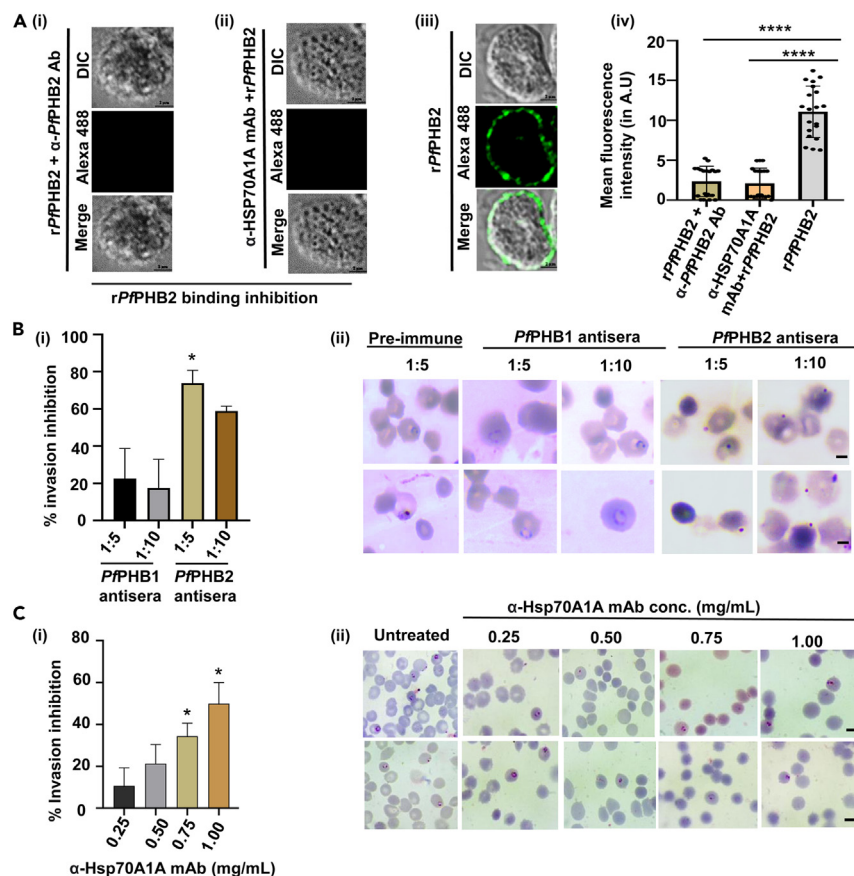
Figure 6. Effect of antibodies targeting Hsp70A1A and *Pf*PHB2 on parasite-RBC binding and merozoite invasion

(A) IFA images probed using anti-*Pf*PHB2 antibody depicting no binding of recombinant *Pf*PHB2 to RBC surface in presence of anti-*Pf*PHB2 antibody (i) and anti-Hsp70A1A monoclonal antibody (ii). (A iii) IFA images showing direct binding of *Pf*PHB2 to RBCs in absence of any antibody (positive control). DIC: differential interference contrast image, Alexa 488: mouse anti-*Pf*PHB2 (green); merge: overlay of *Pf*PHB2 with DIC (Scale bar: 2 μm). (A iv) Intensity of *Pf*PHB2 staining in RBCs under each condition is shown as an intensity graph ($p < 0.0001$****).

(B i) Graph representing percentage invasion inhibition of malaria parasite into normal erythrocytes in the presence of *Pf*PHB1 and *Pf*PHB2 antisera at a dilution of 1:5 and 1:10. Data represent the mean ± SD ($n = 3$) (p values ≤ 0.05*). (B ii) Giemsa-stained images of *Pf*3D7 after treatment with *Pf*PHB1 and *Pf*PHB2 antisera (1:5, 1:10; scale bar: 5 μm) and *Pf*PHB2 preimmune sera.

(C i) Graph representing percentage invasion inhibition of *Pf*3D7 into normal RBCs in the presence of anti-Hsp70A1A monoclonal antibody (0.25 mg/mL, 0.5 mg/mL, 0.75 mg/mL and 1 mg/mL). The experiment was done in triplicate, and the results were shown as mean values ± SD. (p-values ≤ 0.05*) (C ii) Giemsa-stained images of *Pf*3D7 treated with and without anti-Hsp70A1A monoclonal antibodies. Scale bar: 5 μm.

the naive sera was observed in all samples tested (Figure 7A ii). The malaria-infected patient sera was further qualified by coating *Pf*MSP1, a well-characterized merozoite antigen, and taken as positive control in the assay (Figure S8A). To further validate our findings, four patient sera samples showing highest reactivity (P2, P1, P6, P9) in Figure 7A ii were subjected to different dilutions (1: 1,000, 1:2,500, 1:5,000, 1:7,500, 1:10,000) and further tested for reactivity with recombinant *Pf*PHB2. Our data showed that reactivity of recombinant *Pf*PHB2 to the patient sera gradually declines on increasing sera dilution (Figure S8B). Overall, the results suggest the potential of *Pf*PHB2 to provoke immune system to generate antibodies in malaria patients. In light of these results, we checked the expression of *Pf*PHB2 in patient-derived *Plasmodium falciparum* laboratory-adapted line. Rapid detection test positive samples (malaria-infected) were collected from Tripura region from where the patient sera collection was done and adapted under *in vitro* conditions. Immunofluorescence analysis using anti-*Pf*PHB2 antibody depicted the expression of *Pf*PHB2 in these lines (Figure S9).

We next performed antibody neutralization assays to investigate the effect of patient sera on recombinant *Pf*PHB2 binding to RBCs. Here recombinant *Pf*PHB2 was incubated with patient sera showing highest *Pf*PHB2 reactivity (P2) and then allowed to bind with RBCs. Immuno-localization analysis using anti-*Pf*PHB2 antibody depicted no binding of recombinant *Pf*PHB2 to RBC surface (Figure 7B i). Direct binding of recombinant *Pf*PHB2 to RBCs (Figure 7B ii) and neutralization effect of anti-*Pf*PHB2 antibodies on *Pf*PHB2-RBC binding were used as positive control in the assay (Figure 7B iii). No significant neutralizing effect of naive sera was observed on *Pf*PHB2-RBC binding (negative control) (Figure 7B iv). These data clearly suggest the presence of anti-*Pf*PHB2 antibodies in patient sera can block parasite binding to RBCs that
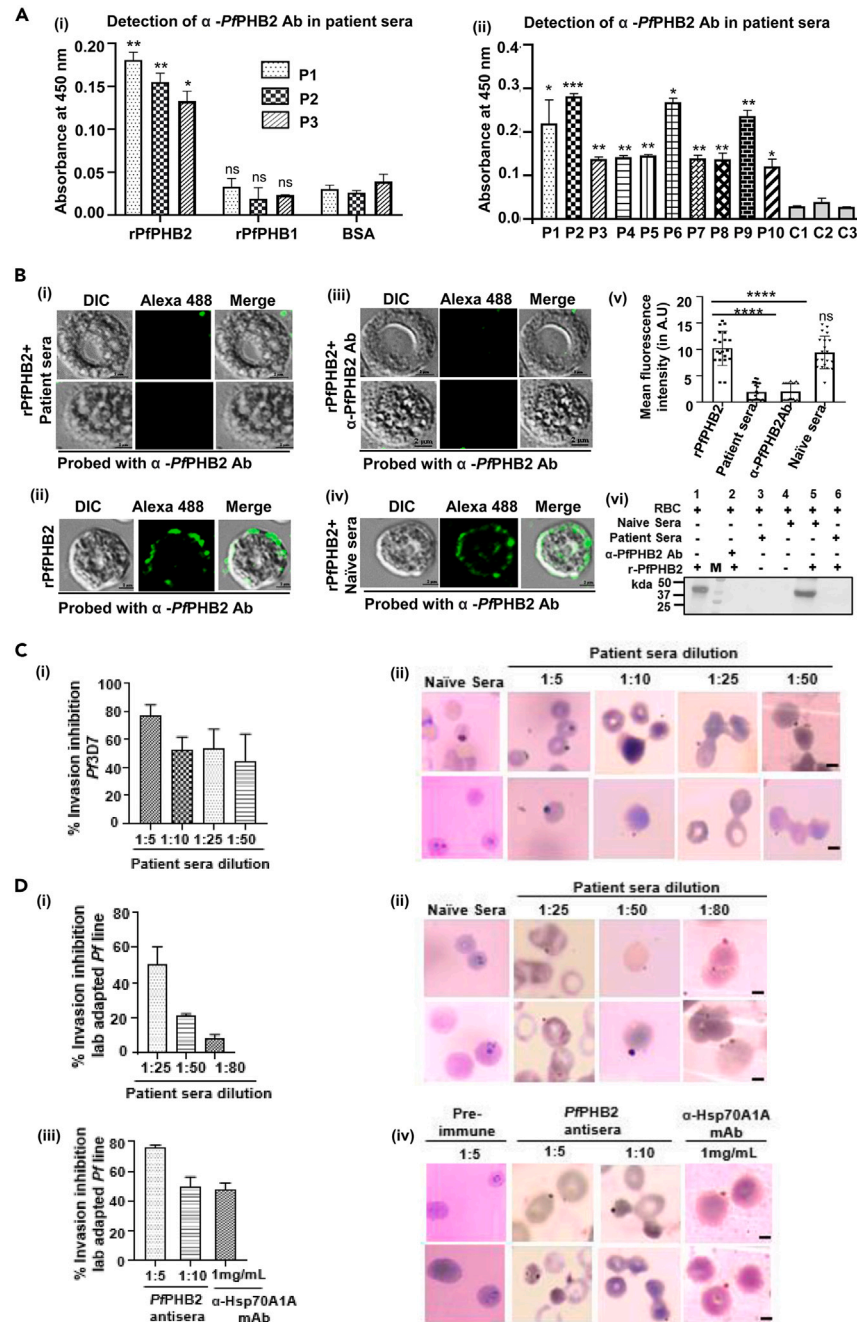
Figure 7. Detection of anti-*Pf*PHB2 antibodies in sera of malaria patients and their effect on *Pf*PHB2-RBC binding and parasite growth

(A i) Semi-quantitative ELISA. 1,000 ng of recombinant *Pf*PHB2, *Pf*PHB1 and BSA were coated on ELISA plates and treated with three different patient sera (1:1,000; P1-P3) followed by secondary human HRP-conjugated antibody (1:10,000). Error bars represent standard deviation among three replicates. Statistical significance is shown with p value ≤0.01** and ≤0.05*. (A ii) Semi-quantitative ELISA. 1,000 ng of recombinant *Pf*PHB2 was coated on ELISA plates and treated with ten different patient sera (1:1,000; P1-P10) and three naive sera (C1-C3) followed by secondary human HRP-conjugated antibody (1:10,000). Error bars represent standard deviation among three replicates. Statistical analysis was performed using unpaired t test and all experimental values were compared with C2. (p value ≤0.001***, p value ≤0.01** and ≤0.05*).

(B) IFA images depicting the effect of patient sera (i) on recombinant *Pf*PHB2 binding to RBCs. Direct binding of recombinant *Pf*PHB2 to RBCs (ii) and neutralization effect of anti-*Pf*PHB2 antibodies (iii) on *Pf*PHB2-RBC binding were taken as positive control while no significant neutralizing effect of naive sera was observed on *Pf*PHB2-RBC binding (negative control) (iv). DIC: differential interference contrast image, Alexa 488: mouse anti-*Pf*PHB2 (green); merge: overlay of *Pf*PHB2 with DIC (Scale bar: 2 μm). (v) Intensity of *Pf*PHB2 staining in RBCs under each condition is shown as an intensity graph (****p < 0.0001). (vi) Western blot analysis showing the neutralizing effect of patient sera on recombinant *Pf*PHB2 binding to RBCs. Recombinant *Pf*PHB2 was incubated with

Figure 7. Continued

patient sera (P2), naive sera (C3) and anti-*Pf*PHB2 antibodies followed by binding to RBCs. Bound protein fractions were eluted and subjected to western blotting with anti-*Pf*PHB2 (1:5000) antibody. Samples are depicted with + and − above each lane.

(C i) Graph showing percentage inhibition of erythrocyte invasion by *Plasmodium falciparum* 3D7 treated with patient sera at different dilutions (1:5, 1:10, 1: 25, and 1:50). Percentage invasion was calculated as follows: % inhibition = (C-T/C) ✕ 100 (C = no. of rings in control [naive sera treated]; T = no. of rings in treatment]).

(C ii) Giemsa-stained images of *Pf*3D7 treated with patient sera (P2) and naive sera (C2) at different dilutions. Scale bar: 5 μm.

(D i, iii) Graph showing percentage inhibition of erythrocyte invasion by patient-derived *Plasmodium falciparum* laboratory-adapted line in presence of patient sera (i) and anti-*Pf*PHB2/Hsp70A1A antibodies (iii) Percentage invasion was calculated as mentioned in C i. (D ii, iv) Giemsa-stained images of patient-derived *Plasmodium falciparum* laboratory-adapted line treated with patient sera (ii) and anti-*Pf*PHB2/Hsp70A1A antibodies (iv). Scale bar: 5 μm.

is mediated by *Pf*PHB2-Hsp70A1A interaction pair. Graph showing mean fluorescence intensity in each case is shown in Figure 7B v. We also performed western blotting to test the neutralizing capacity of patient sera and anti-*Pf*PHB2 antibodies on *Pf*PHB2-RBCs binding. Recombinant *Pf*PHB2 protein was incubated with patient sera (P2), naive sera (C3), and anti-*Pf*PHB2 antibodies and then allowed to bind with RBCs. Bound protein fractions were eluted using NaCl and subjected to western blotting with anti-*Pf*PHB2 (1:5,000) antibody. In presence of patient sera and anti-*Pf*PHB2 antibodies, recombinant *Pf*PHB2 was completely neutralized as no band of ∼32 kDa corresponding to *Pf*PHB2 was observed (Figure 7B vi; lane 6, lane 2, respectively). Band of ∼32 kDa corresponding to *Pf*PHB2 was observed in samples treated with naive sera (Figure 7B vi; lane 5), suggesting the inability of naive sera to neutralize recombinant *Pf*PHB2. RBCs treated with recombinant *Pf*PHB2 showed a band corresponding to ∼32 kDa (positive control; Figure 7B vi; lane 1). RBCs incubated with patient sera and naive sera without recombinant *Pf*PHB2 were also taken as negative controls (Figure 7B vi; lane 3, 4). These results were in accordance with our IFA results in Figure 7B i, ii, iii, and iv.

We performed invasion inhibition assays to further evaluate the effect of patient sera (P2) on the process of merozoite invasion. Schizont-stage culture (1% parasitemia) was treated with patient sera (1:5, 1:10, 1: 25, and 1:50) for 24 h, and the number of new rings formed were counted and compared with the control (naive sera; C2). Our results demonstrated that invasion is significantly inhibited in patient sera-treated parasite culture. An inhibition of 76.96% was observed in case of treatment with patient sera at a dilution of 1:5 (Figure 7C I). Giemsa-stained images of *Pf*3D7 treated with patient and naive sera are shown in Figure 7C ii. These data suggest that patient sera can attenuate the process of merozoite invasion.

Additionally, invasion inhibition assays were performed on patient-derived *Plasmodium falciparum* laboratory-adapted line to evaluate the effect of patient sera (P2) and anti-*Pf*PHB2/anti-Hsp70A1A antibodies. Our results revealed that patient sera significantly reduced the invasion in these lines as compared to naive sera (negative control) (Figure 7D I). Similar results were observed on treatment with anti-*Pf*PHB2 and anti-Hsp70A1A antibodies (Figure 7D iii). Both antibodies significantly inhibit parasite invasion. Preimmune sera (1:5) was taken as negative control for observing the effect of anti-*Pf*PHB2 antibodies while untreated infected RBCs were taken as negative control in case of anti-Hsp70A1A monoclonal antibodies. Giemsa-stained images depicting reduced invasion in treated and control samples are shown in Figure 7D ii, C iv. These data clearly illustrate that patient sera (P2) and anti-*Pf*PHB2/anti-Hsp70A1A antibodies can inhibit the process of merozoite invasion to fresh erythrocytes in patient-derived *Pf* laboratory-adapted line.

DISCUSSION

PHBs that belong to the SPFH superfamily are expressed ubiquitously in all eukaryotic cells, bacteria, and archaea.[3,4] They are known to perform pleiotropic functions ranging from transcription regulation, maintaining mitochondrial structural integrity, senescence, apoptosis to nuclear signaling, cell division, and cellular membrane metabolism. The diverse functions of these membrane-anchored proteins are dependent on their cellular localization and cell type.[7] Owing to their ability to perform numerous functions, PHBs have been regarded as potential targets for therapeutic interventions.[9] In the present study, we have attempted to delineate the unexplored functions of PHBs of malaria parasite with special emphasis to *Pf*PHB2, knowing that the *Pf* PHBs's molecular interactions can help us understand the biology of malaria parasite.

We applied a bacterial two-hybrid screening approach from human cDNA library and identified human Hsp70 "Hsp70A1A" as an interacting partner of *Pf*PHB2. *In vitro* interaction between *Pf*PHB2 and host Hsp70A1A was confirmed by employing a range of protein-protein interaction assays including dot blot, indirect ELISA, and MST. Our MST binding analysis using protein construct spanning SBD of Hsp70A1A depicts similar interaction of *Pf*PHB2 with Hsp70A1A-SBD (K_d value, 2.38 μM) as with full-length Hsp70A1A ($K_{d\ value}$, 1.16 μM). These data demonstrate that *Pf*PHB2-Hsp70A1A binding is mediated through SBD of Hsp70A1A. Our results corroborate those of Jain et al., who had previously reported the binding partner for *Leishmania* PHB on the host cell to be macrophage surface Hsp70.[11]

To get insights into the functional aspect of *Pf*PHB2-Hsp70A1A interaction, we investigated the possibility of receptor-ligand interaction of this pair and tested their role in host cell invasion. Localization analysis of host Hsp70A1A using immunofluorescence assays clearly demonstrates its expression on RBC surface. These results corroborate those of Banumathy et al., who had previously shown that host Chaperones particularly Hsp70, Hsp90, and Hsp60 are recruited in membrane-bound complexes at the surface of the infected erythrocytes by *Plasmodium falciparum*.[22] Fluorescence pattern observed for *Pf*PHB2 is also suggestive of its localization to parasite surface. Our binding assays using recombinant *Pf*PHB2 showed the co-localization of bound *Pf*PHB2 with native Hsp70A1A and further support the interaction of both proteins. We next employed siRNA approach to downregulate the expression of Hsp70A1A in EPCs and investigated whether host Hsp70A1A does indeed play a role in merozoite invasion of human RBCs. Our results demonstrate that merozoite invasion is significantly reduced in Hsp70A1A-specific siRNA-transfected cells as compared to the untransfected control cells, suggesting the involvement of host

Hsp70 during this process. We then performed conditional knockdown of the *Pf*PHB2 gene using glmS ribozyme-mediated approach to study its function in malaria parasite. Synchronized parasite culture grown in the presence of GlcN showed significantly reduced growth. These data suggest that *Pf*PHB2 plays a significant role in parasite survival in human host. We next evaluated the effect of anti-*Pf*PHB2 antisera and anti-Hsp70A1A monoclonal antibody to the binding of recombinant *Pf*PHB2 to RBCs. Our data suggest that *Pf*PHB2-RBC binding is inhibited in the presence of anti-*Pf*PHB2 and anti-Hsp70A1A antibodies. Interestingly, parasite invasion was also blocked by anti-*Pf*PHB2 antisera and anti-Hsp70A1A monoclonal antibody and provides additional evidence for *Pf*PHB2-Hsp70A1A participation in host-parasite interactions.

Host-pathogen interactions mediate disease pathogenesis and parasite development through different stages of its life cycle.[23,24] Successful invasion of *P. falciparum* merozoites to host RBCs involves sequential and coordinated interplay of receptor-ligand interactions.[25] Reports suggest that more than 50 merozoite surface antigens are expressed on *Plasmodium* merozoite surface; however 7−10 possible interactions between them and their erythrocyte receptors are well characterized.[26–28] Erythrocyte-binding proteins (EBPs) and reticulocyte binding-like protein (RH) form two main families of merozoite surface antigens that are known to play crucial role in erythrocyte invasion.[29–31] For example, interaction of parasite ligand PfRh5 with Basigin is known to be essential for invasion by all tested *Plasmodium falciparum* strains.[30,32,33] Previous study by Zenonos et al. has also shown the ability of anti-Basigin antibodies to effectively block erythrocyte invasion by different *Plasmodium* strains.[34] In line with these reports, our study has highlighted an unexplored receptor-ligand complex of *Pf*PHB2-Hsp70A1A that mediates parasite invasion to host erythrocytes.

Multiple stages of the *Plasmodium* parasite's life cycle including sporozoite, RBC-invading merozoite, and asexual blood stages are susceptible to antibodies.[35,36] Also, several reports demonstrated that *Plasmodium* proteins generate antibodies in patients suffering from malaria.[37,38] Our results suggest that *Pf*PHB2 localizes to parasite surface and mediates host-parasite interactions by binding to host Hsp70A1A. In light of the aforementioned facts, we explored vaccine potential of *Pf*PHB2 and tested whether *Pf*PHB2 can elicit antibodies in malaria patients. Our ELISA results indicated the presence of anti-*Pf*PHB2 antibodies in malaria patients that demonstrates immunogenicity of this surface protein and provides an opportunity to use unique epitopes on *Pf*PHB2 molecule in future vaccine design. These results corroborate with those of Dias et al. who reported that PHB of *Leishmania infantum* has the capability to act as a vaccine candidate and diagnostic marker against visceral leishmaniasis.[39] We further performed recombinant *Pf*PHB2-RBC binding assay to explore neutralizing capacity of anti-*Pf*PHB2 antibodies present in patient sera. Our data clearly illustrate the potential of patient sera to inhibit recombinant *Pf*PHB2-RBC binding. Additionally, invasion inhibition assays on *Pf*3D7 demonstrate the ability of patient sera to reduce parasite invasion. These data further hint the potential of anti-*Pf*PHB2 antibodies present in patient sera to affect this critical process. Interestingly, we also tested the effect of patient sera and anti-*Pf*PHB2/anti-Hsp70A1A antibodies on patient-derived *Plasmodium falciparum* laboratory-adapted line. A significant effect of patient sera and anti-*Pf*PHB2/anti-Hsp70A1A antibodies were observed on these lines, highlighting the capability of anti-*Pf*PHB2 and anti-Hsp70A1A antibodies in blocking parasite invasion on laboratory-adapted *Pf* line.

Anti-malarial drugs and vaccine are the current approaches used for global malaria elimination. However a monoclonal antibody approach to abrogate malaria infection is not yet available. Recent reports suggest that human monoclonal antibodies can provide a new approach to decrease malaria morbidity and mortality.[40–42] A study by Gaudinski et al. conducted phase 1 clinical trial to assess the safety and pharmacokinetics of an anti-malarial monoclonal antibody "CIS43LS" and its efficacy against infection with *Plasmodium falciparum*.[40] This report suggested that administration of monoclonal antibody CIS43LS prevented malaria after controlled infection among adults who had never had malaria infection or vaccination.[40] In this regard, our study has also highlighted the potential of anti-Hsp70A1A monoclonal antibody to provide passive prevention against fatal malaria. A previous study by Shevtsov et al. conjugated these Hsp70A1A-specific monoclonal antibody (cmHsp70.1) to superparamagnetic iron nanoparticles to study tumor-specific targeting before and after ionizing irradiation.[43] This report suggests the application of Hsp70-targeted agents in brain tumors owing to the ability of these tumor-specific cmHsp70.1 antibodies targeting Hsp70 present on tumor but not on normal cells.[43] Moreover, these monoclonal antibodies against Hsp70A1A are driven to target SBD of the protein without altering its catalytic ATPase activity. This key feature further highlights its therapeutic importance and its future application with regard to malaria prevention and treatment.

Overall, the data presented here describe a protein pair that participates in host-parasite interaction to mediate *Pf* invasion of RBCs in the blood stage of malaria infections. Based on our findings, we have proposed a model depicting the role of *Pf*PHB2 during the life cycle of malaria parasite (Figure 8). The model demonstrates the possible function of *Pf*PHB2-Hsp70A1A pair during merozoite invasion. Overall, our study demonstrates the capability of *Pf*PHB2 to act as vaccine candidate and proposes monoclonal antibody-based therapeutics targeting host Hsp70A1A for future malaria treatment.

Limitations of the study

The study has elucidated crucial functional roles of *Pf*PHB2 in malaria parasite biology by deciphering its interaction with host Hsp70A1A to facilitate parasite invasion to erythrocytes. The interacting complex of *Pf*PHB2-Hsp70A1A holds a true potential as vaccine candidate as well as invasion-blocking anti-malarial target. However, the present work limits itself with animal-based studies which are essential for potent therapeutics development. Mice model studies can further validate the anti-malarial potential of *Pf*PHB2 antisera and anti-Hsp70A1A monoclonal antibody. Also, purification of immunoglobulin G (IgG) antibodies from anti-*Pf*PHB2 antisera and its testing for invasion-inhibition potential in *Pf*3D7 and other lab-adapted *Pf* lines are another limitation of the study that can further decipher the therapeutic potential of *Pf*PHB2.
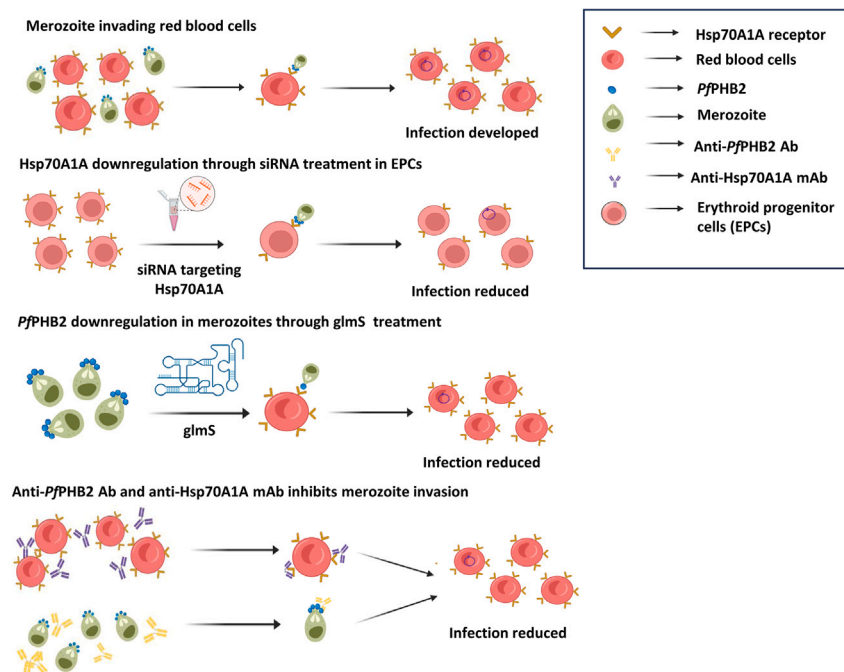
Figure 8. Model depicting the functional role of *Pf*PHB2 during the life cycle of malaria parasite
*Pf*PHB2 interacts with host Hsp70A1A and mediates merozoite invasion to fresh erythrocytes.

STAR★METHODS

Detailed methods are provided in the online version of this paper and include the following:

- KEY RESOURCES TABLE
- RESOURCE AVAILABILITY
  - Lead contact
  - Materials availability
  - Data and code availability
- EXPERIMENTAL MODEL AND STUDY PARTICIPANT DETAILS
  - Parasite culture
- METHOD DETAILS
  - Cloning and bacterial two-hybrid studies of *Pf*PHB1 and *Pf*PHB2
  - Beta galactosidase assay
  - *In silico* docking analysis
  - Cloning, expression, and purification of Hsp70A1A
  - Purification of recombinant *Pf*PHB1 and *Pf*PHB2, and their antibody production
  - Circular dichroism (CD) spectroscopy
  - Dot blot assay
  - Enzyme-linked immunoadsorbant assay (ELISA)
  - Binding assays using Microscale Thermophoresis (MST)
  - Localization of Human Hsp70A1A on RBC surface
  - Immunofluorescence assay for *Pf*PHB2 localization
  - Recombinant *Pf*PHB2 - RBC binding assay
  - Cell culture
  - siRNA transfection against human Hsp70A1A in EPCs
  - Immunofluorescence assay in siRNA transfected EPCs
  - Invasion inhibition assay in siRNA transfected EPCs
  - Cloning and transfection of *Pf*PHB2 gene in *P. falciparum*
  - Western blotting to determine *Pf*PHB2 levels in *Pf*PHB2-HA-glmS transgenic parasites
  - *In vitro* growth assays in *Pf*PHB2 conditional knock down line

- O Antibody neutralization experiments
- O Invasion inhibition assay with anti-*Pf*PHB1/*Pf*PHB2 and anti-Hsp70A1A antibodies and patient sera
- O Western blotting for antibody neutralization assay
- O Quantification and statistical analysis

AUTHOR CONTRIBUTIONS

M.M. and A.B.: experimental design, experimentation, data analysis, and manuscript writing. P.M., M. Saini, and Shreeja Biswas: experiments related to *Pf*PHB2 knockdown using glmS, data analysis, and manuscript writing. R.S.: MST experiments and manuscript preparation. S.G.: experimental design, data analysis, and manuscript writing. G.K., P.G., and S.R.: experiments of siRNA transfection in EPCs. A.M. and S.A.: invasion inhibition assays. A.K.K. and H.T.T.A.: docking studies. Saurav Biswas and I.P.B.: patient sera collection and experiments related to *ex vivo* parasite culture. M. Shevtsov: production of anti-Hsp70A1A monoclonal antibody. A.R. and S.S.: conception of idea, experimental design, data analysis, and manuscript writing.

DECLARATION OF INTERESTS

The authors declare no competing interests.

REFERENCES

1. Organization, W.H.O. (2022). World Malaria Report (2021) (World Health Organization).
2. Fairhurst, R.M., and Dondorp, A.M. (2016). Artemisinin-resistant Plasmodium falciparum malaria. Microbiol. Spectr. *4*. https://doi.org/10.1128/microbiolspec. EI10-0013-2016.
3. Merkwirth, C., and Langer, T. (2009). Prohibitin function within mitochondria: essential roles for cell proliferation and cristae morphogenesis. Biochim. Biophys. Acta -Mol. Cell Res *1793*, 27–32. https://doi.org/10.1016/j.bbamcr.2008.05.013.
4. Browman, D.T., Hoegg, M.B., and Robbins, S.M. (2007). The SPFH domain-containing proteins: more than lipid raft markers. Trends Cell Biol. *17*, 394–402. https://doi.org/10.1016/j.tcb.2007.06.005.
5. Hinderhofer, M., Walker, C.A., Friemel, A., Stuermer, C.A., Möller, H.M., and Reuter, A. (2009). Evolution of prokaryotic SPFH proteins. BMC Evol. Biol. *9*, 1–18. https://doi.org/10.1186/1471-2148-9-10.
6. Signorile, A., Sgaramella, G., Bellomo, F., and De Rasmo, D. (2019). Prohibitins: a critical role in mitochondrial functions and implication in diseases. Cells *8*, 71. https://doi.org/10.3390/cells8010071.
7. Mishra, S., Murphy, L.C., and Murphy, L.J. (2006). The Prohibitins: emerging roles in diverse functions. J. Cell Mol. Med. *10*, 353–363. https://doi.org/10.1111/j.1582-4934.2006.tb00404.x.
8. Tatsuta, T., Model, K., and Langer, T. (2005). Formation of membrane-bound ring complexes by prohibitins in mitochondria. Mol. Bio. Cell *16*, 248–259. https://doi.org/10.1091/mbc.e04-09-0807.
9. Theiss, A.L., and Sitaraman, S.V. (2011). The role and therapeutic potential of prohibitin in disease. Biochim. Biophys. Acta -Mol. Cell Res. *1813*, 1137–1143. https://doi.org/10.1016/j.bbamcr.2011.01.033.
10. Mishra, S., Murphy, L.C., Nyomba, B.G., and Murphy, L.J. (2005). Prohibitin: a potential target for new therapeutics. Trends Mol. Med. *11*, 192–197. https://doi.org/10.1016/j.molmed.2005.02.004.
11. Jain, R., Ghoshal, A., Mandal, C., and Shaha, C. (2010). Leishmania cell surface prohibitin: role in host–parasite interaction. Cell. Microbio. *12*, 432–452. https://doi.org/10.1111/j.1462-5822.2009.01406.x.
12. Mayer, M.P., and Bukau, B. (2005). Hsp70 chaperones: cellular functions and molecular mechanism. Cell. Mol. Life Sci. *62*, 670–684. https://doi.org/10.1007/s00018-004-4464-6.
13. Chakafana, G., Zininga, T., and Shonhai, A. (2019). Comparative structure-function features of Hsp70s of Plasmodium falciparum and human origins. Biophys. Rev. *11*, 591–602. https://doi.org/10.1007/s12551-019-00563-w.
14. Saini, M., Ngwa, C.J., Marothia, M., Verma, P., Ahmad, S., Kumari, J., Anand, S., Vandana, V., Goyal, B., Chakraborti, S., et al. (2023). Characterization of Plasmodium falciparum prohibitins as novel targets to block infection in humans by impairing the growth and transmission of the parasite. Biochem. Pharmacol. *212*, 115567. https://doi.org/10.1016/j.bcp.2023.115567.
15. Altschul, S.F., Madden, T.L., Schäffer, A.A., Zhang, J., Zhang, Z., Miller, W., and Lipman, D.J. (1997). Gapped BLAST and PSI-BLAST: a new generation of protein database search programs. Nucleic Acids Res. *25*, 3389–3402. https://doi.org/10.1093/nar/25.17.3389.
16. Sievers, F., and Higgins, D.G. (2014). Clustal Omega, accurate alignment of very large numbers of sequences. Methods mol. Boil *1079*, 105–116. https://doi.org/10.1007/978-1-62703-646-7_6.
17. Samuchiwal, S.K., Tousif, S., Singh, D.K., Kumar, A., Ghosh, A., Bhalla, K., Prakash, P., Kumar, S., Bhattacharyya, M., Moodley, P., et al. (2014). A peptide fragment from the human COX3 protein disrupts association of

Mycobacterium tuberculosis virulence proteins ESAT-6 and CFP10, inhibits mycobacterial growth and mounts protective immune response. BMC Infect. Dis. *14*, 1–11. https://doi.org/10.1186/1471-2334-14-355.

18. Jumper, J., Evans, R., Pritzel, A., Green, T., Figurnov, M., Ronneberger, O., Tunyasuvunakool, K., Bates, R., Žídek, A., Potapenko, A., et al. (2021). Highly accurate protein structure prediction with AlphaFold. Nature *596*, 583–589. https://doi.org/10.1038/s41586-021-03819-2.

19. Satchwell, T.J. (2022). Generation of red blood cells from stem cells: achievements, opportunities and perspectives for malaria research. Front. Cell. Infect. Microbiol. *12*, 1039520. https://doi.org/10.3389/fcimb.2022.1039520.

20. Prommana, P., Uthaipibull, C., Wongsombat, C., Kamchonwongpaisan, S., Yuthavong, Y., Knuepfer, E., Holder, A.A., and Shaw, P.J. (2013). Inducible knockdown of Plasmodium gene expression using the glmS ribozyme. PLoS One *8*, e73783. https://doi.org/10.1371/journal.pone.0073783.

21. Chan, J.A., Fowkes, F.J., and Beeson, J.G. (2014). Surface antigens of Plasmodium falciparum-infected erythrocytes as immune targets and malaria vaccine candidates. Cell. Mol. Life Sci. *71*, 3633–3657. https://doi.org/10.1007/s00018-014-1614-3.

22. Banumathy, G., Singh, V., and Tatu, U. (2002). Host Chaperones Are Recruited in Membrane-bound Complexes by Plasmodium falciparum. J. Biol. Chem. *277*, 3902–3912. https://doi.org/10.1074/jbc.M110513200.

23. Acharya, P., and Garg, M. (2017). Host–parasite interactions in human malaria: clinical implications of basic research. Front. Microbiol. *8*, 263186. https://doi.org/10.3389/fmicb.2017.00889.

24. Su, X.Z., Zhang, C., and Joy, D.A. (2020). Host-malaria parasite interactions and impacts on mutual evolution. Front. Cell. Infect. Microbiol. *10*, 587933. https://doi.org/10.3389/fcimb.2020.587933.

25. Wright, G.J., and Rayner, J.C. (2014). Plasmodium falciparum erythrocyte invasion: combining function with immune evasion. PLoS Pathog. *10*, e1003943. https://doi.org/10.1371/journal.ppat.1003943.

26. Weiss, G.E., Gilson, P.R., Taechalertpaisarn, T., Tham, W.H., de Jong, N.W., Harvey, K.L., Fowkes, F.J., Barlow, P.N., Rayner, J.C., Wright, G.J., et al. (2015). Revealing the sequence and resulting cellular morphology of receptor-ligand interactions during Plasmodium falciparum invasion of erythrocytes. PLoS Pathog. *11*, e1004670. https://doi.org/10.1371/journal.ppat.1004670.

27. Tham, W.H., Lim, N.T., Weiss, G.E., Lopaticki, S., Ansell, B.R., Bird, M., Lucet, I., Dorin-Semblat, D., Doerig, C., Gilson, P.R., et al. (2015). Plasmodium falciparum adhesins play an essential role in signalling and activation of invasion into human erythrocytes. PLoS Pathog *11*, e1005343. https://doi.org/10.1371/journal.ppat.1005343.

28. Salinas, N.D., and Tolia, N.H. (2016). Red cell receptors as access points for malaria infection. Curr. Opin. Hematol. *23*, 215–223.

29. Tham, W.H., Healer, J., and Cowman, A.F. (2012). Erythrocyte and reticulocyte binding-like proteins of Plasmodium falciparum. Trends Parasitol. *28*, 23–30. https://doi.org/10.1016/j.pt.2011.10.002.

30. Crosnier, C., Bustamante, L.Y., Bartholdson, S.J., Bei, A.K., Theron, M., Uchikawa, M., Mboup, S., Ndir, O., Kwiatkowski, D.P., Duraisingh, M.T., et al. (2011). Basigin is a receptor essential for erythrocyte invasion by Plasmodium falciparum. Nature *480*, 534–537. https://doi.org/10.1038/nature10606.

31. Harvey, K.L., Gilson, P.R., and Crabb, B.S. (2012). A model for the progression of receptor–ligand interactions during erythrocyte invasion by Plasmodium falciparum. Int. J. Parasitol. *42*, 567–573. https://doi.org/10.1016/j.ijpara.2012.02.011.

32. Douglas, A.D., Baldeviano, G.C., Lucas, C.M., Lugo-Roman, L.A., Crosnier, C., Bartholdson, S.J., Diouf, A., Miura, K., Lambert, L.E., Ventocilla, J.A., et al. (2015). A PfRH5-based vaccine is efficacious against heterologous strain blood-stage Plasmodium falciparum infection in aotus monkeys. Cell Host Microbe *17*, 130–139. https://doi.org/10.1016/j.chom.2014.11.017.

33. Ord, R.L., Caldeira, J.C., Rodriguez, M., Noe, A., Chackerian, B., Peabody, D.S., Gutierrez, G., and Lobo, C.A. (2014). A malaria vaccine candidate based on an epitope of the Plasmodium falciparum RH5 protein. Malar. J. *13*, 1–9. https://doi.org/10.1186/1475-2875-13-326.

34. Zenonos, Z.A., Dummler, S.K., Müller-Sienerth, N., Chen, J., Preiser, P.R., Rayner, J.C., and Wright, G.J. (2015). Basigin is a druggable target for host-oriented antimalarial interventions. J. Exp. Med. *212*, 1145–1151. https://doi.org/10.1084/jem.20150032.

35. Richards, J.S., Stanisic, D.I., Fowkes, F.J., Tavul, L., Dabod, E., Thompson, J.K., Kumar, S., Chitnis, C.E., Narum, D.L., Michon, P., et al. (2010). Association between naturally acquired antibodies to erythrocyte-binding antigens of Plasmodium falciparum and protection from malaria and high-density parasitemia. Clin. Infect. Dis. *51*, 50–60. https://doi.org/10.1086/656413.

36. Dobbs, K.R., and Dent, A.E. (2016). Plasmodium malaria and antimalarial antibodies in the first year of life. Parasitol *143*, 129–138. https://doi.org/10.1017/S0031182015001626.

37. Wipasa, J., Suphavilai, C., Okell, L.C., Cook, J., Corran, P.H., Thaikla, K., Liewsaree, W., Riley, E.M., and Hafalla, J.C.R. (2010). Long-lived antibody and B Cell memory responses to the human malaria parasites, Plasmodium falciparum and Plasmodium vivax. PLoS Pathog. *6*, e1000770. https://doi.org/10.1371/journal.ppat.1000770.

38. Julien, J.P., and Wardemann, H. (2019). Antibodies against Plasmodium falciparum malaria at the molecular level. Nat. Rev. Immunol. *19*, 761–775. https://doi.org/10.1038/s41577-019-0209-5.

39. Dias, D.S., Ribeiro, P.A., Martins, V.T., Lage, D.P., Ramos, F.F., Dias, A.L., Rodrigues, M.R., Portela, Á.S., Costa, L.E., Caligiorne, R.B.,

et al. (2018). Recombinant prohibitin protein of Leishmania infantum acts as a vaccine candidate and diagnostic marker against visceral leishmaniasis. Cell. Immunol. *323*, 59–69. https://doi.org/10.1016/j.cellimm.2017.11.001.

40. Gaudinski, M.R., Berkowitz, N.M., Idris, A.H., Coates, E.E., Holman, L.A., Mendoza, F., Gordon, I.J., Plummer, S.H., Trofymenko, O., Hu, Z., et al. (2021). A monoclonal antibody for malaria prevention. N. Engl. J. Med. *385*, 803–814. https://doi.org/10.1056/NEJMoa2034031.

41. Kayentao, K., Ongoiba, A., Preston, A.C., Healy, S.A., Doumbo, S., Doumtabe, D., Traore, A., Traore, H., Djiguiba, A., Li, S., et al. (2022). Safety and efficacy of a monoclonal antibody against malaria in Mali. N. Engl. J. Med. *387*, 1833–1842. https://doi.org/10.1056/NEJMoa2206966.

42. Lyke, K.E., Berry, A.A., Mason, K., Idris, A.H., O'Callahan, M., Happe, M., Strom, L., Berkowitz, N.M., Guech, M., Hu, Z., et al. (2023). Low-dose intravenous and subcutaneous CIS43LS monoclonal antibody for protection against malaria (VRC 612 Part C): a phase 1, adaptive trial. Lancet Infect. Dis. *23*, 578–588. https://doi.org/10.1016/S1473-3099(22)00793-9.

43. Shevtsov, M.A., Nikolaev, B.P., Ryzhov, V.A., Yakovleva, L.Y., Marchenko, Y.Y., Parr, M.A., Rolich, V.I., Mikhrina, A.L., Dobrodumov, A.V., Pitkin, E., et al. (2015). Ionizing radiation improves glioma-specific targeting of superparamagnetic iron oxide nanoparticles conjugated with cmHsp70. 1 monoclonal antibodies (SPION–cmHsp70.1). Nanoscale *7*, 20652–20664. https://doi.org/10.1039/c5nr06521f.

44. Miller, J.H. (1972). Experiments in Molecular Genetics (Cold Spring Harbor Laboratory Pr).

45. Madhavi Sastry, G., Adzhigirey, M., Day, T., Annabhimoju, R., and Sherman, W. (2013). Protein and ligand preparation: parameters, protocols, and influence on virtual screening enrichments. J. Comput. Aided Mol. Des. *27*, 221–234. https://doi.org/10.1007/s10822-013-9644-8.

46. Jacobson, M.P., Pincus, D.L., Rapp, C.S., Day, T.J., Honig, B., Shaw, D.E., and Friesner, R.A. (2004). A hierarchical approach to all-atom protein loop prediction. Proteins: Struct., Funct., Bioinf. *55*, 351–367. https://doi.org/10.1002/prot.10613.

47. Schindelin, J., Rueden, C.T., Hiner, M.C., and Eliceiri, K.W. (2015). The ImageJ ecosystem: An open platform for biomedical image analysis. Mol. Reprod. Dev. *82*, 518–529. https://doi.org/10.1002/mrd.22489.

48. Anam, Z.E., Joshi, N., Gupta, S., Yadav, P., Chaurasiya, A., Kahlon, A.K., Kaushik, S., Munde, M., Ranganathan, A., and Singh, S. (2020). A De novo peptide from a high throughput peptide library blocks myosin A-MTIP complex formation in Plasmodium falciparum. Int. J. Mol. Sci. *21*, 6158. https://doi.org/10.3390/ijms21176158.

49. Kurita, R., Suda, N., Sudo, K., Miharada, K., Hiroyama, T., Miyoshi, H., Tani, K., and Nakamura, Y. (2013). Establishment of immortalized human erythroid progenitor cell lines able to produce enucleated red blood cells. PLoS One *8*, 59890. https://doi.org/10.1371/journal.pone.0059890.

STAR★METHODS

KEY RESOURCES TABLE

REAGENT or RESOURCE	SOURCE	IDENTIFIER
Antibodies		
Goat anti-Mouse IgG (H + L) Cross-Adsorbed Secondary Antibody, Alexa Fluor™ 488	Invitrogen™	Cat # A-11001; RRID: AB_2534069
Goat anti-Rabbit IgG (H + L) Cross-Adsorbed Secondary Antibody, Alexa Fluor™ 594	Invitrogen™	Cat # A-11012; RRID: AB_2534079
Mouse anti-Histidine primary monoclonal Antibody	Thermoscientific	Cat # PA1-983B; RRID: AB_1069891
Rabbit anti-Mouse IgG1 Secondary Antibody, HRP	Thermoscientific	Cat # PA1-86329; RRID: AB_933678
GAPDH-HRP conjugated	Abclonal	Cat # AC035; RRID: AB_2769863
Chemicals, peptides, and recombinant proteins		
RPMI Medium 1640	Gibco™	Cat # 23400013
2-Phenylethyl beta-D-thiogalactoside	Sigma-Aldrich	Cat #P4902
5-Bromo-4chloro-3indoxyl-beta-D-galactopyronoside (X-gal Substrate)	G-Biosciences	Cat #R1233
Bovine Serum Albumin, BSA	Sisco Research Laboratory (SRL)	Cat # 97350
Freund's Complete Adjuvants	Sigma-Aldrich	Cat #F5881
Freund's incomplete Adjuvants	Sigma-Aldrich	Cat #F5506
o-Nitrophenyl-beta-D-Galactopyranoside (o-NPG)	Sigma-Aldrich	Cat # 45-N1127
Ni-NTA Resin	G-Biosciences	Cat # 786-90
Precision plus protein dual color standard	Bior-Rad	Cat # 1610374
N-Acetyl-D-glucosamine	Sigma-Aldrich	Cat # A3286
ProLong™ Gold Antifade Mountant with DAPI	Invitrogen™	Cat #P36935
Arabinose	Sisco Research Laboratory (SRL)	Cat # 52392
IPTG	Thermoscientific	Cat #R0392
Protein Assay Dye	Bio-Rad	Cat # 5000006
Critical commercial assays		
TMB substrate kit	Thermoscientific	Cat # 34021
ECL Western Blotting Substrates kit	Bio-Rad	Cat # 1705060
Monolith Protein Labeling Kit RED-NHS 2ND Generation (Amine Reactive)	nanoTEMPER	Cat # MO-L011
Experimental models: Organisms/strains		
Plasmodium falciparum 3D7 strain	Malaria Research and Reference Reagent Resource Center (MR4)	NA
Software and algorithms		
ImageJ	NIH	https://imagej.nih.gov/ij; RRID: SCR_003070
Graphpad Prism	GraphPad Prism Software	https://www.graphpad.com/scientific-software/prism; RRID: SCR_002798
Biorender	NA	https://www.biorender.com/; RRID: SCR_018361

RESOURCE AVAILABILITY

Lead contact

Further information and requests for resources and reagents should be directed to and will be fulfilled by the lead contact, Prof. Shailja Singh (Shailja.jnu@gmail.com).

Materials availability

This study did not generate new unique reagents.

Data and code availability

- The published article and supplemental information include all data generated and analyzed during this study.
- This paper does not report original code.
- Any additional information supporting the current study in this paper is available from the lead contact upon request.

EXPERIMENTAL MODEL AND STUDY PARTICIPANT DETAILS

Parasite culture

Briefly, *P. falciparum* 3D7 parasites were grown in complete RPMI 1640 medium (containing 2 mM/L-glutamine, 25 mM HEPES) supplemented with 2 g/L sodium bicarbonate (Sigma, USA), 50 mg/L hypoxanthine (Sigma, USA) and 5 g/L Albumax I (Gibco, USA), pH 7.4 using O+ human RBCs at 2% hematocrit. Parasite culture was maintained in a mixed gas environment (90% N_2, 5% CO_2 and 5% O_2). Parasites were synchronized in consecutive two cycles by 5% sorbitol treatment at the ring stage. Culture parasitemia levels were monitored by staining the smears with Giemsa and visualizing the cells under 100 X by light microscopy.

METHOD DETAILS

Cloning and bacterial two-hybrid studies of *Pf*PHB1 and *Pf*PHB2

Full length *Pf*PHB1 and *Pf*PHB2 were codon-optimized and synthesized in pUC57 through GenScript. *Pf*PHB1 and *Pf*PHB2 inserts were excised from pUC57 and cloned in SnaBI restriction enzyme digested and dephosphorylated pTRGnn and pBTnn vectors. The positive clones were selected by colony PCR and confirmed by plasmid restriction digestion and nucleotide sequencing. Bacterial two-hybrid experiments were performed as described by the manufacturer's protocol (Stratagene, San Diego, CA, USA). The human cDNA library, cloned into the pTRG vector, was acquired commercially from Stratagene, CA, USA (Catlog: 982201). Briefly, equal amounts of pTRG containing the human cDNA library and pBT containing the *Pf*PHB2 gene plasmids (250 ng each) were used to co-transform R1 reporter cells. The cells were plated on X-gal indicator plates, containing kanamycin (50 μg/mL), tetracycline (12.5 μg/mL), chloramphenicol (30 μg/mL), X-gal (80 μg/mL), X-gal inhibitor 2-phenylethyl-β-D-thiogalactoside (200 μM), isopropyl β-D-1-thiogalactopyranoside (25 μM), and incubated at 30°C for 48 h. The blue-colored colonies indicated a positive interaction. A previously known interaction of Mtb proteins ESAT6 and CFP10 that has also been established by the bacterial two-hybrid system and yields blue-colored colonies upon co-transformation was used as a positive control[18]; ESAT6/empty pBTnn, which yielded white-colored colonies, was used as a negative control. Finally, the partner pBTnn and pTRGnn plasmids were sequenced and BLAST analysis was performed to identify the interacting protein.

Beta galactosidase assay

To quantitatively assess the strength of interaction between *Pf*PHB2 and Hsp70A1A, the expression of a β-D-galactosidase reporter enzyme was measured by a colorimetric assay.[44] Briefly, the selected interacting co-transformant and the corresponding negative controls were grown to mid-log phase in the presence of 40 μM IPTG. Induction was carried out using 0.2% Arabinose at A_{600} and culture was allowed to grow for 3 h at 37°C. 500 μL aliquot of cultures were pelleted down and washed with 1mL Z buffer (60 mM $Na_2H_2PO_4$, 40 mM NaH_2PO_4, 10 mM KCl, 1 mM $MgSO_4$, pH = 7.4). 150μL of Z buffer along with 40 mM β-mercaptoethanol (β-ME), 50μL chloroform, 20μL of 0.1% SDS was added with vigorous mixing followed by addition of 200μL *o*-nitrophenyl-β-D-galactoside (ONPG; 4 mg/mL) substrate. Cells were incubated with the substrate at 30°C for 30 mints. 0.5 mL 1M Na_2CO_3 was added to stop the reaction followed by recording of optical density at 420 nm. Statistical significance was assessed using two-tailed unpaired Student's t test by comparing all values to the negative control (pBTnn-ESAT6 negative interaction). Enzyme activity in miller units (M.U) was calculated as follows.

$$Enzyme\ activity\,(M.U)\ =\ \frac{1000\ *\ O.D_{420}}{Time\,(mints)\ *\ Volume\ (ml)\ *\ O.D_{600}}$$

In silico docking analysis

The crystal structure of human Hsp70 (PDB ID: 4WV5) at 2.04 Å resolution was retrieved from the Protein DataBank (PDB). The predicted structures of *Pf*PHB1 and *Pf*PHB2 were retrieved from AlphaFold Protein Structure Database.[18] Both structures were validated through Ramachandran plot and protein reliability report in Schrodinger suites 2023-4. All the protein structures were loaded as PDB files in Schrödinger 2023-4 and prepared with the embedded Protein Preparation Wizard application (Schrodinger, LLC, NY, USA, 2009)[45,46] using default settings, i.e.,

adding hydrogens, assigning disulfide bonds, removing surrounding waters, adjusting charges, capping termini, and adding missing side chains using Prime. The optimization of hydrogen bonds was performed to resolve structural ambiguities, and a final restrained minimization of the system was carried out under the OPLS4 force field. In greater detail, a full optimization for hydrogen atoms and a 0.30 Å maximum RMSD deviation from the initial position for the heavy atoms were allowed. To evaluate the protein–protein complex interactions protein–protein rigid docking approach was employed using the PIPER module of Schrodinger maestro. Briefly, (Human Hsp70) was selected as the receptor and PfPHB1, PfPHB2 as ligands, and the number of ligand rotations to the probe box (1 Å) was set at 70,000 (maximum), which corresponds approximately to sampling every 5° in the space of Euler angles. The step size of the translational grid was 1 Å. The resulting poses were ranked by the size of the cluster from the rigid ligand docking results. Maximum cluster generation was set up at 30 in our case; hence top 30 docked poses were produced.

Cloning, expression, and purification of Hsp70A1A

The full length Hsp70A1A gene (641 amino acids) was codon-optimized for bacterial expression and synthesized commercially (Gene Script USA) in pUC57 vector, with the gene cloned at the unique SnaBI restriction site. Hsp70A1A gene was excised and cloned in, SnaBI-cut de-phosphorylated pMTSAra plasmid. This was followed by the screening of clones using gene and vector-specific primers (Hsp70A1A For/ pBAD Rev). Hsp70A1A-pMTSAra, upon induction, expresses with a C-terminal hexaHistidine tag (Hsp70A1A-His6x). To obtain large scale his-tagged protein, BL21 cells carrying Hsp70A1A-pMTSA plasmid were grown in liquid culture overnight at 37°C with streptomycin (50 μg/μL). Later secondary culture was inoculated with 1% inoculum and grown till mid-log phase in the presence of streptomycin and induced with 0.2% arabinose for 5 h at 37°C with constant shaking. Cells were collected and the pellet washed with 1XPBS (pH 7.4), following which it was resuspended in lysis buffer (50 mM Tris, 150 mM NaCl, pH 7.4, 2 mM PMSF) and sonicated till a clear lysate was obtained. The lysate was centrifuged at 13000 rpm for 1 h. The lysate was allowed to bind Ni-NTA beads overnight at 4°C, and the protein was subsequently purified by slowly increasing imidazole concentration in 20 mM Tris, 100 mM NaCl. The eluted fractions were run on 10% SDS-PAGE, and the fractions having high concentrations of the protein were pooled and subsequently dialyzed against PBS pH 7.4. The purified protein was run on 10% SDS-PAGE and confirmed by Western blot analysis using anti-Histidine antibodies (1:5000 dilution).

SBD region of Hsp70A1A (annotated as Hsp70A1A-SBD) was cloned in pMTSAra plasmid and expressed in bacterial expression system. Here SBD was PCR amplified from full length codon-optimised gene of Hsp70A1A present in pUC57 using SBD specific primers. Amplified product was digested with SnaBI and cloned in SnaBI-cut dephosphorylated pMTSAra plasmid. Protein purification was performed using 0.2% arabinose induction in 2 L of culture. The cell biomass was sonicated in a re-suspension buffer (50 mM Tris-Cl, 10 mM EDTA pH 7.5) in the presence of Protease Inhibitor Cocktail, (PIC) (1X) and phenylmethylsulfonyl floride (PMSF) (2 mM) until a clear solution was obtained. Inclusion bodies were pelleted down at 13000 rpm for 30 min 4°C. Pellet was washed with buffer containing 50 mM Tris HCl, 100 mM NaCl, 0.5% triton-100 and 0.1% sodium azide at 13000 rpm for 10 min. To remove Triton from pellet it was again washed with only 50 mM Tris-cl and 100 mM Nacl. The washed pellet then dissolved in solubilization buffer having 6M GuHCl, 10mMTris pH 8.0, 300 Mm NaCl overnight at RT. The insoluble bodies were removed by spinning at 13000 rpm for 20 min. The collected supernatant was incubated with equilibrated Ni-NTA beads for 2 hrs at RT on a rotor shaker. Resins were then packed onto a column followed by 10 volume of washing with 20 mM imidazole made in 8M urea, 20 mM Tris-Cl, 500 mM NaCl pH 8.0. Elute fractions were collected at 50 mM, 150 mM, 250 mM of imidazole concentration and then run on 15% SDS-PAGE.

Purification of recombinant PfPHB1 and PfPHB2, and their antibody production

Recombinant PfPHB1 and PfPHB2 were purified for experiments and polyclonal antisera were generated against both proteins as described.[14] Briefly, codon optimized PfPHB1 and PfPHB2 were cloned in pMTSAra plasmid and expressed in bacterial expression system. Protein purification was performed using 0.2% arabinose for induction. The cell biomass was sonicated in a re-suspension buffer (30 mM Tris-Cl, 0.5 mM EDTA pH 7.5) in the presence of Protease Inhibitor Cocktail, (PIC) (1X) and phenylmethylsulfonyl floride (PMSF) (2 mM) until a clear solution was obtained. Inclusion bodies were pelleted down and washed with buffer containing 50 mM Tris HCl, 100 mM NaCl, 0.5% triton-100 and 0.1% sodium azide followed by washing with buffer having 50 mM Tris-Cl and 100 mM NaCl. The washed pellet was then dissolved in solubilisation buffer (6M GuHCl, 10 mM Tris pH 8.0, 300 Mm NaCl) for overnight at RT. The insoluble bodies were removed by spinning at 13000 rpm for 20 min. Protein was purified from supernatant fraction using Ni-NTA affinity chromatography.

For anti-PfPHB1 and anti-PfPHB2 polyclonal antibody production, male BALB/c mice were used. 0.5mL of pre-immune sera was collected at Day 0 and antigen emulsion having 50 μg of recombinant proteins with Complete Freund's Adjuvant was injected subcutaneously. Post this, mice were given three booster doses at an interval of 14 days. Booster doses were prepared with 25 μg antigen dosage in Incomplete Freund's Adjuvant. Final bleed was collected at day 62.

Circular dichroism (CD) spectroscopy

The far-UV CD spectra were collected on PfPHB1, PfPHB2, Hsp70A1A and Hsp70A1A-SBD by chiarascan using 1 mm cuvette. All four proteins were diluted to 0.2 mg/ml concentration in phosphate buffer, pH 7.4 and collected the CD data in 260 to 200 nm wavelength range with 1 nm bandwidth and 40 nm/min scanning rate. Five scans were collected for each data and averaged. The baseline was subtracted from the averaged CD data. The CD (mdeg) was plotted against wavelength.

Dot blot assay

5 µg each of recombinant *Pf*PHB1, *Pf*PHB2 and BSA (negative control) were immobilized on the nitrocellulose membrane followed by blocking with 5% BSA overnight at 4°C. Post washing, blot was hybridized with Hsp70A1A (5 µg/mL in 1% BSA/PBST) for 2 h at room temperature. After extensive washing, blots were incubated with anti-Hsp70A1A monoclonal antibody (1:5000 dilution) for 1 h followed by horseradish peroxidise (HRP)-conjugated goat anti-mouse secondary antibody (1:5000). Blot was developed using ECL substrate (Biorad). Integrated densities of dots were measured using ImageJ after background correction.[47]

Enzyme-linked immunoadsorbant assay (ELISA)

ELISA-based protein–protein interaction assay was carried out, as described previously,[48] with slight modifications. Briefly, 200 ng of recombinant *Pf*PHB2 (dissolved in 100µL of carbonate/bicarbonate buffer) was coated on ELISA plates overnight at 4°C and blocked with 5% BSA in PBS for 2 h at 37°C. After extensive washing with 1XPBST (1 × PBS, 0.05% Tween 20), plates were incubated with increasing concentrations of Hsp70A1A (-250 ng, 500 ng, 1000 ng, 2000 ng, 4000 ng, 6000 ng) for 2 h at 37°C. BSA was incubated with Hsp70A1A as a negative control. Overlaid bound protein was detected by incubating anti-Hsp70A1A monoclonal antibody (1:30,000) for 2 h followed by horseradish peroxidase (HRP)-conjugated anti-mice secondary antibody (1:30000) for 1 h. Washed plated were developed by incubating 3'3',5,5'-Tetramethylbenzidine (TMB) substrate at 37°C for 15–30 min until color development. The reaction was stopped by adding 2N H_2SO_4, and the absorbance was recorded at 450 nm

    Similar protocol was followed to detect the presence of *Pf*PHB2 antibodies in patient sera. Sera from active malaria patients were obtained from Regional Medical Research Center (RMRCNE), Dibrugarh, India, and was originally collected from Dhalai district of Tripura region.

    Sera from active malaria patients were obtained with the consent of patients and in case of minors from their parents/guardians as approved by the Institutional Bio-safety Committee (IBSC) of the Jawaharlal Nehru University (JNU/IBSC/2020/17) and Institutional Ethics Committee of Agartala Govt. Medical College, Agartala [F.4-(6–13) AGMC/Medical Education/IEC Approval/2022). 1000 ng of recombinant *Pf*PHB2 (dissolved in 100 uL of carbonate/bicarbonate buffer) was coated on ELISA plates and blocked with 5% BSA in PBS for 2 h at 37°C. After extensive washing with 1XPBST, the coated ligand was incubated with patient sera (P1 to P10; 1:1000) and with naive sera (C1 to C3; 1:1000) for 2 h at 37°C. Washed plates were incubated with anti-*Pf*PHB2 (1:5000) followed by anti-mice HRP conjugated secondary antibodies (1:10,000) for 2 h. Plates were developed using TMB substrate.

Binding assays using Microscale Thermophoresis (MST)

The kinetic measurements of *Pf*PHB2-Hsp70A1A and *Pf*PHB2-Hsp70A1A-SBD binding was performed using Monolith NT.115 instrument (NanoTemper Technologies, Munich, Germany). 10 µM Hsp70A1A and Hsp70A1A-SBD were labeled using 30 µM Lysine reactive dye (Monolith Series Protein Labeling Kit RED-NHS 2nd Generation) and incubated for 30 min. The concentration of labeled Hsp70A1A and Hsp70A1A-SBD protein were kept constant at a concentration of 50 nM and 2.2 µM respectively. The unlabeled binding partner *Pf*PHB2 (25 µM) was serially diluted in decreasing concentrations and titrated against constant concentration of the labeled Hsp70A1A in 1:1 dilution. Samples were diluted in 1x PBS/0.01% Tween 20 buffer and incubated for 15 min at room temperature, followed by centrifugation at 8000 rpm for 10 min at room temperature. The samples were taken into the capillaries (K002 Monolith NT.115) and thermophoretic mobility was analyzed. Data evaluation was performed with the Monolith software (Nano Temper, Munich, Germany). The Kd is estimated by fitting the equation:

$$F(c_{ligand}) = Unbound + (Bound - Unbound) \cdot \frac{c_{ligand+}\ c_{target} + K_d\ -\ \sqrt{(c_{ligand}+c_{target}+K_d)^2 - 4 \cdot c_{ligand} \cdot c_{target}}}{2c_{target}}$$

where $f(c_{ligand})$ is the Fnorm value at a given ligand concentration c_{ligand};
    Unbound is the Fnorm signal of the target alone;
    Bound is the Fnorm signal of the complex;
    Kd is the dissociation constant or binding affinity;
    and c_{target} is the final concentration of target in the assay.

Localization of Human Hsp70A1A on RBC surface

Thin blood smears of 1X PBS washed uninfected human RBCs were fixed in methanol for 45 min at −20°C, permeablized with 0.05% PBS/Tween 20, and blocked with 5% (w/v) BSA in PBS. Mouse anti-Hsp70A1A monoclonal (1:500) primary antibody were added and incubated for 2 h at room temperature. Alexa Fluor 488 conjugated goat anti-mouse (1:500, green color; Invitrogen) were used as secondary antibodies. The slides were analyzed using a confocal microscope. For co-localization studies, anti-Hsp70A1A-FITC conjugated monoclonal (1:300) antibody and mice anti-Band 3 primary antibodies (1:200) were used. Alexa Fluor 594 conjugated anti-mice (1:500, red color, Invitrogen, Carlsbad, CA, USA) were used as secondary antibodies.

Immunofluorescence assay for *Pf*PHB2 localization

Thin blood smears of mixed stage *Pf*3D7 cultures at 5% parasitaemia were fixed in methanol for 45 min at −20°C, permeablized with 0.05% PBS/Tween 20, and blocked with 5% (w/v) BSA in PBS.Mouse anti-*Pf*PHB2 (1:300) primary antibodies were added and incubated

for 2 h at room temperature. Alexa Fluor 488 conjugated anti-mouse (1:500, green color; Invitrogen) were used as secondary antibodies. The parasite nuclei were counterstained with DAPI (40, 60-diamidino- 2-phenylindole; Invitrogen, USA). The slides were examined using a confocal microscope (Olympus, Shinjuku, Tokyo, Japan) with a 100✗ oil immersion objective. For co-localization studies, mouse anti-PfPHB2 (1:300) and rabbit anti-PfMSP1 (1:300) were added as primary antibodies. Alexa Fluor 594 conjugated anti-rabbit (1:500, red color, Invitrogen, Carlsbad, CA, USA) and Alexa Fluor 488 conjugated anti-mouse (1:500, green color; Invitrogen) were used as secondary antibodies.

Recombinant PfPHB2 - RBC binding assay

Uninfected human erythrocytes (1.5×10^8 cells) were washed with incomplete RPMI media and incubated with 10 µg recombinant PfPHB1/PfPHB2 in incomplete RPMI media for 2 h followed by fixation with PFG (4% paraformaldehyde +0.0075% glutaraldehyde) and subsequent blocking with 5% BSA. Cells were incubated with anti-PfPHB2 mice sera (1:200) and then with anti-mice alexa-flour 488 secondary antibody (1:500). Cells were washed, drop casted on slides, and visualized using confocal microscopy. For co-localization studies of recombinant PfPHB2 and native Hsp70A1A, anti-Hsp70A1A-FITC conjugated monoclonal antibody (1:300) were used.

Cell culture

Erythroid progenitor cells (EPCs) were maintained as described previously with minor modifications.[49] Briefly, cells were cultured in expansion medium (StemSpan SFEM II (Stemcell Technologies Inc.), 50 ng/mL SCF (Immunotools, Germany), 3 U/ml EPO (Peprotech, India) and 10−6 M dexamethasone (Sigma-Aldrich)), along with 1 µg/mL of 1-doxycycline (Sigma-Aldrich). The cells were maintained in this medium at a density of $1-3 \times 10^5$ cells/ml at 37 °C, 5% CO_2. Culture medium was changed 2–3 times per week and replaced with fresh medium. HEK293T cells were maintained in DMEM high glucose medium (GIBCO) supplemented with 10% FBS (GIBCO) and 1X anti-biotic and anti-mycotic solution (Sigma-Aldrich). The cells were maintained at 37 °C in incubator supplemented with 5% CO_2.

siRNA transfection against human Hsp70A1A in EPCs

For knockdown of human Hsp70A1A expression in EPCs, pro-erythroblast staged cells were transfected with siRNA designed against Hsp70A1A (Thermo Fischer, siRNA ID: 108236) at two different concentration (100 nM and 250 nM). 0.5×10^6 EPCs were electroporated at 1100 V, 30 ms, 3 pulses using the Neon Transfection system (Thermo Fisher Scientific) as per the manufacturer's protocol. After 6 h post transfection, cells were washed with 1X PBS and re-suspended in expansion medium. After 72 h of transfection, the cells were harvested and analyzed for Hsp70A1A expression by Immunofluorescence assay.

Immunofluorescence assay in siRNA transfected EPCs

IFA was performed to assess the expression of Hsp70A1A in EPCs after gene knockdown. siRNA transfected cells were smeared onto glass slide and fixed with chilled methanol for 30 min at −20°C. Slides were then blocked for 1 h at room temperature (RT) in 3% bovine serum albumin (BSA) prepared in 1X PBST. After blocking, slides were incubated with anti-Hsp70A1A (1:1000) for 1 h at RT. Slides were then washed with 1X PBST twice, followed by probing with Alexa Fluor (AF)-488 conjugated goat anti-rabbit IgG (1:500 dilution; Molecular Probes, United States) at RT for 1 h. Slides were then washed again and mounted with Pro Long Gold antifade reagent (Invitrogen, Carlsbad, CA, United States) and viewed under fluorescence microscope (Olympus) at 60✗ magnification.

Invasion inhibition assay in siRNA transfected EPCs

Percoll purified schizonts at 1% parasitemia and 2% hematocrit were incubated with progenitor cells transfected with Hsp70A1A targeted siRNA (100 nM and 250 nM) in a volume of 100µL. The assay plates were incubated at 37°C under mixed gas conditions for 24 h and the number of new rings formed were scored by observing thin Giemsa stained smears of each assay well. Percentage invasion was calculated as follows: (Infected cells/total no of cells) ✗ 100.

Cloning and transfection of PfPHB2 gene in P. falciparum

Selected coding region of PfPHB2 (358–912 bp) was used to clone the sequences in HA-glmS plasmid at BglII/PstI restriction digestion sites. The plasmid constructs were confirmed with restriction digestion with respective restriction enzymes followed by sequencing the plasmids to validate the constructs. To generate genetically modified P. falciparum cell lines, 3D7 parasites were transfected with the plasmids. 100 µg of plasmid were precipitated in 10 µL 3 M NaOAc (pH 5) and 250 µL absolute ethanol followed by incubation at −20°C overnight. The plasmid DNA was pelleted at 10000 rpm, 4°C for 20 min, washed with 1 mL 70% ethanol and air dried followed by dissolving the pellet in 15 µL pre-warmed TE buffer and 385 µL prewarmed Cytomix buffer (120 mM KCl, 0.15 mM $CaCl_2$, 10 mM K_2HPO_4, 10 mM KH_2PO_4, 25 mM HEPES, 2 mM EGTA, 5 mM $MgCl_2$, dH_2O up to 100 mL, pH 7.6). P. falciparum 3D7 with parasitemia ≥5% predominantly at ring stages were pelleted and the prepared plasmid DNA was added to the cells and transferred to an electroporation cuvette. The transfected cells were placed in a 25 cm^3-tissue culture flask with 5 mL complete RPMI medium with human erythrocytes with a hematocrit of 5%. Following 6–24 h, the medium was replaced with appropriate selection medium (WR99210 for HA-glmS/HAM-9). The cultures were

regularly checked for growth through smears stained with Giemsa. Genomic DNA from the parasites was isolated to verify the genetic manipulation through PCR.

Western blotting to determine *Pf*PHB2 levels in *Pf*PHB2-HA-glmS transgenic parasites

To detect the down-regulation of *Pf*PHB2 in *Pf*PHB2-HA-glmS line, ∼ 4% ring stage culture was synchronised using 5% sorbitol. Synchronized culture at the early trophozoite stage was treated with 2.5 mM glucosamine for 8 h at 37°C. Treated and untreated cultures were harvested and incubated with 0.1% Saponin (in PBS) for 10 min on ice and centrifuged at 4,000 rpm for 10 min at 4°C followed by washing with 1X PBS. Purified parasites were subjected to RIPA lysis using two volume of RIPA lysis buffer (30 mM Tris, 150 mM NaCl, 20 mM MgCl$_2$, 1 mM EDTA, 1 mM β-ME, 0.5% Triton X-100, 1% IGEPAL, 1 mM PMSF, and 0.1% SDS; pH 8.0). The lysate was further quantified by bicinchoninic acid protein assay. Samples were separated on 12% SDS-PAGE and subjected to western blotting using anti-*Pf*PHB2 antisera (1:200) followed by anti-mice HRP conjugated secondary antibody (1:5000). HRP-conjugated GAPDH mouse monoclonal antibody (1:5000) were used to detect GAPDH as loading control. Blots were developed by ECL (enhanced chemiluminescence) reagent.

In vitro growth assays in *Pf*PHB2 conditional knock down line

*Pf*PHB2-HA-glmS transgenic parasites were tightly synchronized with 5% sorbitol and grown with media containing 2.5 mM concentration of glucosamine (GlcN) (Sigma -Aldrich) for 96 h. Media was changed on daily basis containing glucosamine. Parasites of thin blood films were stained with Giemsa and around ∼2000 red blood cells (RBCs) were counted under 100× objective of light microscope. Total parasitaemia of *Pf*PHB2-HA-glmS transgenic line treated with GlcN was compared with the control (without glucosamine).

Antibody neutralization experiments

To evaluate the effect of anti-*Pf*PHB2, anti-Hsp70A1A monoclonal antibodies on recombinant *Pf*PHB2 binding to RBCs, we performed antibodies neutralization assays. Here, anti-*Pf*PHB2 antibodies (1:50) were incubated with 10 μg recombinant *Pf*PHB2 overnight at 4°C. Uninfected human erythrocytes (1.5 ×10^8 cells) were washed with incomplete RPMI media followed by incubation with recombinant *Pf*PHB2 - anti-*Pf*PHB2 antibodies reaction mixture. RBCs were fixed with PFG and subsequently blocked with BSA before probing with anti-*Pf*PHB2 antibodies (1:300) and anti-mice alexa-flour 488 secondary antibody (1:500) for 2 h. Cells were visualized using confocal microscopy. In second set of reaction, anti-Hsp70A1A monoclonal antibodies (1:100) were incubated with RBCs for 1 h followed by incubation with recombinant *Pf*PHB2 (10 μg). RBCs were fixed with PFG and subsequently blocked with 5% BSA before probing with anti-*Pf*PHB2 antibodies (1: 300) and anti-mice alexa-flour 488 secondary antibody (1: 500).

Similarly, these experiments were performed to evaluate the effect of patient sera on *Pf*PHB2- RBC binding. Here, patient sera with highest *Pf*PHB2 reactivity (1:50) and naive sera were incubated with 10 μg recombinant *Pf*PHB2 separately overnight at 4°C. Uninfected human erythrocytes (1.5 ×10^8 cells) were washed with incomplete RPMI media followed by incubation with recombinant *Pf*PHB2 – patient sera/naive sera reaction mixture.

Invasion inhibition assay with anti-*Pf*PHB1/*Pf*PHB2 and anti-Hsp70A1A antibodies and patient sera

The antisera used for invasion inhibition assay was heat inactivated by heating at 60°C for 20 min in order to inactivate the complement proteins. Percoll purified schizonts at 1% parasitemia and 2% hematocrit were incubated in the presence of *Pf*PHB1 and *Pf*PHB2 antisera at a dilution of 1:5 and 1:10 and anti-Hsp70A1A monoclonal antibody (0.25, 0.5, 0.75 and 1 mg/mL) in a volume of 100μL. The assay plates were incubated at 37°C under mixed gas conditions for 24 h and the number of new rings formed were scored by observing thin giemsa stained smears of each assay well. Similarly, parasite culture (schizonts; 1% parasitemia) was treated with different dilutions of patient sera (1:5, 1:10, 1:25 and 1:50) and seeded in a 96 well plate. The assay plates were incubated at 37°C under mixed gas conditions for 24 h and the number of new rings formed were counted. Parasite culture was treated with different dilutions of naive sera (1:5, 1:10, 1:25 and 1:50) as a negative control. Percentage invasion inhibition was calculated as follows: % inhibition = (C-T/C) ×100.

C = no. of rings in control (preimmune sera in case of *Pf*PHB1 and *Pf*PHB2 antisera treatment and uninfected RBCs in case of anti-Hsp70A1A monoclonal antibody treatment); T = no. of rings in treatment).

Similarly, invasion inhibition assays with anti-*Pf*PHB2/anti-Hsp70A1A antibodies and patient sera were performed on patient derived *Pf* laboratory adapted line. Blood from malaria infected patients were collected from Dhalai district of Tripura region from where the patient sera collection was done following taking informed consent from each patient as approved by the Institutional Bio-safety Committee (IBSC) of the Jawaharlal Nehru University (JNU/IBSC/2020/17) and Institutional Ethics Committee of Agartala Govt. Medical College, Agartala [F.4-(6–13) AGMC/Medical Education/IEC Approval/2022]. Rapid detection test positive samples (malaria infected) were collected and adapted under *in vitro* conditions. Species confirmation was performed by PCR using 18s rRNA primers. Percoll purified schizonts at 1% parasitemia and 2% hematocrit were incubated in the presence of *Pf*PHB2 antisera (1:5 and 1:10), Hsp70A1A monoclonal antibody (1 mg/ml) and patient sera (1:25, 1:50, 1:80). The assay plates were incubated for 24 h and the number of new rings formed were counted. Percentage invasion inhibition was calculated as mentioned above.

Western blotting for antibody neutralization assay

10 μg of recombinant *Pf*PHB2 protein was incubated with naive sera, patient sera and anti-*Pf*PHB2 antibodies for overnight at 4°C. Post incubation, reaction mixtures were allowed to bind with RBCs (1.5×10^8) for 2 h at room temperature. Bound protein fractions were eluted by treating RBCs with 1.5M NaCl for 10 mints at 4°C. The supernatant having the bound protein was separated by centrifugation at 6000 rpm for 15 min and run on 12% SDS-gel followed by western blotting with anti-*Pf*PHB2 (1:5000) antibody.

Quantification and statistical analysis

All data are shown as mean ± SD. Statistical difierences were determined using Student's unpaired 2-tailed t-test. All statistics were performed using GraphPad Prism Version 8.0 (GraphPad Software, USA). $p \leq 0.05$ was considered significant.